Current Research in Biotechnology 4 (2022) 102–119

Contents lists available at ScienceDirect

Current Research in Biotechnology

journal homepage: www.elsevier.com/locate/crbiot

Model-assisted DoE applied to microalgae processes

Veronika Gassenmeier [a,1], Sahar Deppe [a,c,1], Tanja Hernández Rodríguez [a,1], Fabian Kuhfuß [a,f], André Moser [e], Volker C. Hass [e], Kim B. Kuchemüller [b], Ralf Pörtner [b], Johannes Möller [b], George Ifrim [a,d], Björn Frahm [a,*]

[a] Ostwestfalen-Lippe University of Applied Sciences and Arts, Biotechnology & Bioprocess Engineering, Lemgo, Germany
[b] Hamburg University of Technology, Institute for Bioprocess and Biosystems Engineering, Hamburg, Germany
[c] Fraunhofer Institute of Optronics, System Technologies and Image Exploitation IOSB, Industrial Automation branch INA, Lemgo, Germany
[d] Dunarea de Jos University of Galati, Department of Automatic Control and Electrical Engineering, Galati, Romania
[e] Furtwangen University of Applied Sciences, Institute of Applied Biology, Faculty of Medical and Life Sciences, Villingen-Schwenningen, Germany
[f] Rentschler Biopharma SE, Production and Manufacturing, Laupheim, Germany

ARTICLE INFO

Keywords:
DoE
Model-assisted
mDoE
Algae
Mathematical process model
Light intensity
Desmodesmus pseudocommunis
Chlorella vulgaris

ABSTRACT

This study assesses the performance of the model-assisted Design of Experiment (mDoE) software toolbox for the design of two microalgae bioprocesses. The mDoE-toolbox was applied to maximize biomass growth for *Desmodesmus pseudocommunis* in a photobioreactor by varying the light intensity and pH and for *Chlorella vulgaris* in shake flasks, by varying the light intensity and duration. For both case studies, a mathematical mechanistic model was applied. In the first study only one experiment was necessary to adapt the mathematical model and identify a combination of light intensity and pH that improved biomass yield, as confirmed experimentally. In the second study, no well-established model was available for the specific experimental arrangement. On the basis of the literature, a mathematical model was constructed and a first cycle of mDoE was performed, thus identifying the desired factor combinations. Experiments confirmed the high biomass yield but revealed shortcomings of the model. The model was improved and a second cycle of mDoE was performed. The recommended factor combinations from both cycles were comparable. The mDoE was found to be a time-saving, cost-effective and useful method enabling the identification of factor combinations leading to high biomass production for the design of two different microalgae bioprocesses with low experimental effort.

1. Introduction

Biotechnological processes are subject to numerous influences thus making the development and establishment of new processes cost-, time- and labor-intensive. Temperature, pH, oxygen concentration, stirring speed and variable components in the media are some of the influential factors that must be considered in the experimental design and, therefore, investigated in a wide variety of combinations. Such investigation would require a large number of experiments to determine the appropriate levels of the process parameters (Béchet et al., 2017; Qiu et al., 2017; Gatamaneni et al., 2018). One-factor-at-a-time approaches demand a lot of effort, because instead of changing several parameters simultaneously, only one factor is tested each time.

In contrast, Design of Experiments (DoE) approaches are more effective. The mode of operation of DoE involves identifying correlations between critical process parameters and their influence on the final target, e.g., the product concentration or productivity (Tao et al., 2020). Drawbacks of DoE methods include the reduction of complex bioprocesses to a few key performance indicators, such as the final product concentration, while neglecting the dynamics of growth and metabolism (Möller et al., 2019; Kuchemüller et al., 2020). Additionally, still many experiments have to be performed and evaluated with DoE methods (Moser et al., 2021).

To further decrease the number of experiments required and to enable knowledge-driven bioprocess development, a model-assisted DoE software providing an efficient toolbox for bioprocess design and -optimization has recently been introduced (Möller et al., 2019).

Abbreviations: DoE, Design of Experiments; mDoE, model-assisted Design of Experiments.

* Corresponding author.
E-mail address: bjoern.frahm@th-owl.de (B. Frahm).
URL: http://www.th-owl.de (B. Frahm).

[1] Equal first authorship.

https://doi.org/10.1016/j.crbiot.2022.01.005

Model-assisted Design of Experiments (mDoE) combines statistical DoE with mechanistic modeling by using mathematical process models to simulate most of the recommended experiments, instead of performing all experiments in the laboratory. These simulations are then treated in the DoE as performed experiments thus enabling the creation of a well-defined experimental space in DoE, without a need to perform all the designed experiments. Thus, the number of experiments is substantially decreased (Moser et al., 2021).

Mathematical process models are a crucial part of mDoE and for several knowledge-driven bioprocess development strategies (Glassey et al., 2011; von Stosch et al., 2016; Möller et al., 2019; Kuchemüller et al., 2020). For phototrophic microalgae, multiple models have been published for different experimental situations, e.g., different types of photobioreactors (PBRs), cultivation in open ponds under natural daylight conditions, cultivation in reactors using artificial light sources, (Tamiya et al., 1953; Yun and Park, 2003; Aslan and Kapdan, 2006; Mairet et al., 2010; Filali et al., 2011; Concas et al., 2012; He et al., 2012; Eze et al., 2018). Most of these models use Monod kinetics to account for substrate limitations and photolimitation (Béchet et al., 2013). Some models apply an inhibition term for algal species in which photo-inhibition is observed (Béchet et al., 2014; Ifrim et al., 2014). When modeling phototrophic growth, accounting for the light shielding caused by the growing biomass concentration is particularly challenging and is usually implemented by the calculation of decreasing local light intensities along the light path. A widely used approach to solve this problem is to compute light attenuation by using the Lambert–Beer equation (Béchet et al., 2013). To compute the influence of the local light intensities on the entire system, an average light intensity is calculated by integration along the light path, which then affects the growth rate (Béchet et al., 2014), or various local growth rates are computed along the light path and the average growth rate is then determined (Ifrim et al., 2014).

Building on the existing process models, the aim of this study was to test whether the new method using the mDoE-toolbox could be used successfully applied to process development in the field of algae cultivation. The mDoE-approach, to date, has been included in a software tool and tested for antibody-producing Chinese hamster ovary cell culture (Möller et al., 2020), yeast cultivation and whole cell biocatalysis (Moser et al., 2021). To analyze the performance of the mDoE-approach in microalgae processes, we performed two case-studies for microalgae bioprocesses by using three different mathematical process models.

In the first case study, case study A (CSA), a simplified variant of the complex model published in Ifrim et al. (2014), was used as a mathematical process model for mDoE. The model was previously validated (Ifrim et al., 2014) and was used to evaluate the applicability of mDoE-toolbox to phototrophic organisms in a laboratory flat-plate PBR. The aim of CSA was to maximize the biomass growth of *Desmodesmus pseudocommunis* (*D. pseudocommunis*), while varying the factors pH and light intensity.

In the second case study, case study B (CSB), shake flask cultivation of *Chlorella vulgaris* was chosen to maximize biomass yield in a fixed time span, while varying the intensity and duration of lighting. The laboratory scale using shake flasks was chosen because it provides the flexibility to perform multiple parallel experiments with different cultivation conditions (e.g., with respect to light) and thus supports the development of a suitable model. The experimental arrangement in CSB comprised a shaker with adjustable lighting of the individual shake flasks from below in an incubator with a regulated CO_2 atmosphere and constant temperature. For this experimental arrangement, no validated mathematical model was available. A first cycle of mDoE was performed by using a simple model setup based on literature sources. In CSB, a second cycle of mDoE was performed after modification of the model, partially on the basis of the knowledge acquired in the first cycle of mDoE. The outcomes of mDoE from both cycles were compared.

2. Materials and Methods

2.1. Experiments and analytics - D. pseudocommunis in photobioreactor (CSA)

Cultivation conditions and measurements:. The strain of *D. pseudocommunis* used in PBR cultivation was obtained from the Institute of Biological Research, Cluj-Napoca, Romania. The microalgae were cultivated in a modified Bold Basal Medium containing $NaHCO_3$ (1.68 $g\,L^{-1}$), NH_4Cl (1.45 $g\,L^{-1}$), $MgSO_4{\cdot}7H_2O$ (0.28 $g\,L^{-1}$), $CaCl_2{\cdot}2H_2O$ (0.05 $g\,L^{-1}$), KH_2PO_4 (0.175 $g\,L^{-1}$), H_3BO_3 (0.0114 $g\,L^{-1}$), EDTA-Na_2-KOH (1 mL of the stock solution with 5 g/100 mL EDTA-Na_2 and 3.1 g/100 mL KOH), $FeSO_4{\cdot}7H_2O$-H_2SO_4 (1 mL of the stock solution with 4.98 g/100 mL $FeSO_4{\cdot}7H_2O$ and 1 mL of H_2SO_4) and 1 mL of trace elements solution (according to BBM recipe (Bischoff and Bold, 1963; Andersen, 2005)). The concentration of biomass X was measured daily by filtering 10 mL of culture and weighting it after approximately 24 h of drying in an oven at 110 °C. The dried biomass was measured in triplicate. In addition, the concentrations of total nitrogen and phosphorus were measured to confirm that the growth was not limited.

Experiments:. Batch experiments of *D. pseudocommunis* were performed in a flat-plate air-lift laboratory PBR (cf. Fig. 1). The PBR had a working volume of 5 L with a culture depth of 5.4 cm. The artificial light was provided by a LED grow light panel on one side of the reactor equipped with transparent polycarbonate panels. The PBR contained sensors for pH, temperature, dissolved oxygen, dissolved carbon dioxide and turbidity. It also accommodated nozzles for gas addition and feed and culture evacuation, a septum for sampling with a syringe, and a condenser.

The LED grow light panel consisted in five LED grow light chips containing diodes for the entire visible spectrum, focusing on photosynthetic active wavelengths to enhance growth. The photosynthetic active radiation ($\mu mol\,m^{-2}s^{-1}$) emitted by the light panel was measured with a LI-COR LI-190R quantum sensor in μmol photon $m^{-2}s^{-1}$ and generates up to 1400 $\mu mol\,m^{-2}s^{-1}$. The light field generated by the panel was heterogeneous and thus the average incident light intensity was calculated by measuring the incident light at 25 points on the lighted surface, as described in Ifrim et al. (2019). The light panel was dimmable and could be controlled by the process computer between 0 and 8 V, thus being calibrated for any desired average incident light intensity (I_0), which was one of the experimental factors in this case study.

The second experimental factor was the pH which was monitored by a probe sensor (Mettler Toledo InPro 3253i). The pH was controlled by addition of CO_2 into the microalgae culture to decrease the pH. To enable pH control, the culture medium was buffered with bicarbonate. At a lower pH (i.e., 6.5), the chemical equilibrium of the bicarbonate-water system slowly shifted towards CO_2 which was consumed by the microalgae. When all bicarbonate was depleted (i.e., converted to CO_2) pH control was no longer possible, because the pH of the medium without bicarbonate was approximately 5.

In the air-lift reactor, the homogenization was performed by sparging gas into the culture. Because CO_2 addition was insufficient for mixing, a constant flow of N_2 gas was added (i.e., 20 $mL\,min^{-1}$). Air could have been used instead, but then the measurement of the dissolved oxygen derived from photosynthesis would have been impossible. The addition of N_2 had a stripping effect on the dissolved gases (dissolved O_2 from photosynthesis and dissolved CO_2). Stripping the dissolved CO_2 from the culture required additional CO_2 to regulate the pH (dissolved from the bubbled CO_2 gas and converted from the bicarbonate through thermodynamic equilibrium) thus providing an effective mechanism to maintain a constant pH throughout batch cultivation. The gasses were added to the reactor by means of a ceramic fine bubble diffuser (DY 101CC-SERIES, AngelAqua, Busan, South

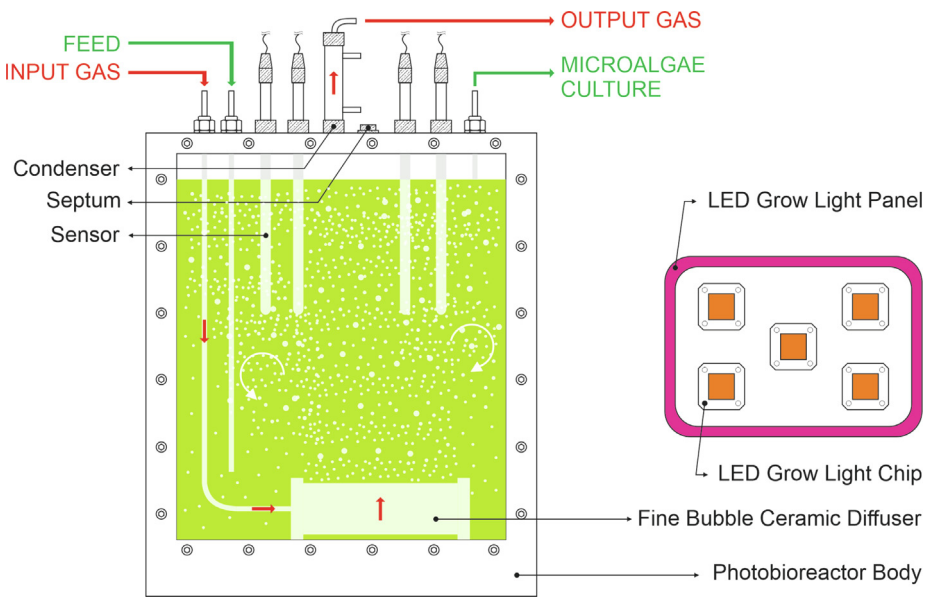

Fig. 1. Setup of the Air-lift laboratory PBR and its mounted LED grow light panel used for the cultivation of *D. pseudocommunis* (CSA).

Korea) and measured and controlled by two Bronkhorst High Tech EL-FLOW BASE mass flow meters with control valves, with measurement ranges of 0–100 $mL\,min^{-1}$ for N_2 and 0–20 $mL\,min^{-1}$ for CO_2. The concentration of dissolved oxygen was monitored with a Mettler Toledo InPro 6850i polarographic sensor and the concentration of dissolved carbon dioxide was monitored with a Mettler Toledo InPro 5000i sensor. The signals of the sensors were translated by Mettler Toledo M800 adapters into 0–10 V analog signals. A dSpace board acquired all signals from the sensors, flowmeters and the LED grow light panel and stored them in databases on the computer.

Throughout the batch process, the system was thus able to maintain constant average incident light intensity, I_0, and pH, thus enabling the formulation of a bivariate optimization problem.

The *D. pseudocommunis* microalgae were cultivated at room temperature (between 27 and 31 °C (Vanags et al., 2015)) because the polycarbonate panels of the PBR did not allow for the installation of a temperature regulation system.

The incident light intensity, I_0, was maintained at 400 (experiment #1), 602 (experiment #2) and 795 (experiment #3) $\mu mol\,m^{-2}s^{-1}$, and the pH was 6.5 (experiments #1 and #2) or 7 (experiment #3).

2.2. Experiments and analytics - C. vulgaris in shake flasks (CSB)

Cultivation conditions and measurements: The strain of *C. vulgaris* used in experiments was obtained from the Collection of Algae Cultures of the University of Göttingen (SAG, Germany). For cultivation, the media proposed by Kessler and Czygan (1970) was modified on the basis of the results of Mandalam and Palsson (1998). The modified medium consisted of: KNO_3 (3.00 $g\,L^{-1}$), NaCl (0.47 $g\,L^{-1}$), $NaH_2PO_4 \cdot 2H_2O$ (0.47 $g\,L^{-1}$), $Na_2HPO_4 \cdot 12H_2O$ (0.36 $g\,L^{-1}$), $MgSO_4 \cdot 7H_2O$ (0.4 $g\,L^{-1}$), $CaCl_2 \cdot 2H_2O$ (0.014 $g\,L^{-1}$), $FeSO_4 \cdot 7H_2O$ (0.006 $g\,L^{-1}$), $MnCl_2 \cdot 4H_2O$ (0.0005 $g\,L^{-1}$), H_3BO_3 (0.0005 $g\,L^{-1}$), $ZnSO_4 \cdot 7H_2O$ (0.0002 $g\,L^{-1}$), $(NH_4)_6MO_7O_{24} \cdot 4H_2O$ (0.00002 $g\,L^{-1}$), EDTA-Na_2 (0.008 $g\,L^{-1}$), H_2O (double distilled) (1000 mL). The suppliers of all components are listed in Table A.1 in the Appendix.

Experiments: Experiments were conducted in narrow-necked and unbaffled glass shake flasks (VWR, Radnor, Pennsylvania, USA) with a volume of 500 mL. As a sterile barrier, "Silicosen Type Super" (Hirschmann Laborgeraete GmbH and Co. KG, Eberstadt, Germany) steril plugs were used. The flasks were shaken on a MaxQ 2000 CO_2 (Thermo Fisher Scientific, Waltham, Massachusetts, USA) orbital shaker at 100 rpm (shaking diameter: 19 mm) with a mounted custom lighting tablet (Almostec GmbH, Perchtoldsdorf, Austria). The photosynthetically active radiation was adjustable between 300 and 1200 $\mu mol\,m^{-2}s^{-1}$ and controllable via timers. The temperature was set to 25 °C, and the CO_2 was set to 5% (V/V) according to commonly used settings described in the literature (Mallick et al., 2011; Chinnasamy et al., 2011). Each flask for the cultivation of *C. vulgaris* was inoculated with a starting biomass concentration of $X_0 = 0.1\ g\,L^{-1}$ and a total working volume of 200 mL. Biomass concentration X was measured by the optical density at $\lambda = 740$ nm, according to the correlation between the dry biomass X and the optical density determined previously. All measurements were performed in triplicates.

Samples of 7.5 mL were collected and replaced with medium to ensure a constant working volume. To determine the nitrate concentration in the samples (c_N in $g\,L^{-1}$), the method of Cataldo et al. (1975) was used. The pH was measured with a pH-meter (WTW, Weilheim, Germany). Additionally, the chlorophyll (a + b) and carotenoid concentrations were monitored using the extraction via methanol as described by Miazek and Ledakowicz (2013) and Wellburn (1994). These measurements were used to survey possible metabolic changes in the algae, as can occur with substrate limitation, but also with light damage (bleaching), during cultivation under various light intensities and durations.

3. Theory and Calculations

3.1. Mathematical models

3.1.1. Model for D. pseudocommunis (CSA)

Microalgae in CSA were cultivated in a PBR with constant lateral lighting and controlled pH. The mathematical model used for the growth of microalgae in a PBR is fairly complex and was previously published in Ifrim et al. (2014). The global photosynthetic growth model associates three sub-models: a radiative model able to describe the attenuation of light inside the culture, a biological model that describes the main state variables of the aquatic and gaseous systems and a thermodynamic model that quantifies all molecular and ionic species of the NH_3 - CO_2 - H_2O multi-solute system. The thermodynamic model is an excellent tool to calculate and simulate the pH of the culture. The model was previously validated on a strain of *Chlamy-*

domonas reinhardtii cultivated in a torus shaped PBR (Ifrim et al., 2014). The adaptation of the model to *D. pseudocommunis* cultivated on a flat-plate PBR with small modification of the parameters makes it a reliable benchmark for the cultivation of microalgae in photoautotrophic growth conditions with regulation of pH and lighting.

With the pH considered an independent variable (i.e., experimental factor), the global photoautotrophic growth model can be simplified by eliminating the thermodynamic model. Because the growth of microalgae is expressed as a function of light intensity and pH (two independent variables), the equation describing the biomass concentration can be decoupled from the rest of the model and can serve as a simple and reliable tool in the mDoE-process. The simplified model consists of a single differential equation for biomass concentration.

$$\frac{dX}{dt} = \mu\, X - \mu_D\, X \tag{1}$$

The specific growth rate μ, expressed as a function of light availability inside the culture (i.e., irradiance) and pH has the following form:

$$\mu = \mu_{max}\ \frac{1}{L}\int_0^L f(I(z))\, dz\, f(\mathrm{pH}), \tag{2}$$

where L is the depth of the PBR. The specific growth rate is averaged over various depth according to Cornet and Dussap (2009) to address various local light intensities. A new empirical model that describes the kinetic of light inhibition was investigated through the following equation:

$$f(I(z)) = \frac{(I_{max} - I_{opt})(I(z) - I_{min})}{(I_{opt} - I_{min})(I_{max} - I(z))} e^{1 - \frac{(I_{max} - I_{opt})(I(z) - I_{min})}{(I_{opt} - I_{min})(I_{max} - I(z))}} \tag{3}$$

The advantage of this model over the conventional inhibition model, (as introduced in Andrews (1968) and still currently used (Lee et al., 2015)), is that the optimal irradiance I_{opt} is easy to handle (Cornet and Dussap, 2009; Ifrim et al., 2014). In addition, the parameters I_{min} and I_{max} can easily be identified because they are the limits of the irradiance range in which the microalgae can grow (I_{min} is clearly zero). Given the advantages of this model over the conventional inhibition model, we used it with Eq. (2) in this case study. The expression of the radiative model, explained in detail in Cornet and Dussap (2009), is:

$$I(z) = I_0\ e^{-\frac{(1+\alpha)}{2\alpha} E_a\, X\, z} \tag{4}$$

with $\alpha = \sqrt{\frac{E_a}{E_a + 2bE_s}}$, mass absorption coefficient E_a, mass scattering coefficient E_s and back scattering fraction b.

The function describing the influence of the pH on the specific growth rate has the following expression:

$$f(\mathrm{pH}) = \frac{\mathrm{pH} - \mathrm{pH}_{min}}{\mathrm{pH}_{max} - \mathrm{pH}}\ e^{1 - \frac{\mathrm{pH} - \mathrm{pH}_{min}}{\mathrm{pH}_{max} - \mathrm{pH}}} \tag{5}$$

where pH_{min} and pH_{max} are the pH-range in which the microalgae can grow. The optimal pH is between the two parameters.

3.1.2. Initial model (Model 1) for C. vulgaris (CSB)

In the literature, some models for PBRs have considered light intensity, but must be adjusted to the particular experimental setting (Gatamaneni et al., 2018; Fernández-Sevilla et al., 2018; Lee et al., 2015; Eilers and Peeters, 1988).

The initial model based on the literature consists of two differential equations for biomass concentration X and volume V. The change in biomass concentration over time depends on the specific growth rate (μ), death rate (μ_D) and a term accounting for dilution when medium (F_M) is added (see Eq. (6a)). The differential equation for the volume (V) includes the volume reduction when samples are collected (F_S) and the volume increase due to the addition of fresh medium (F_M) (Eq. (6b)).

The Monod kinetics for the specific growth rate μ, depending on the average light intensity I_{avg} as the substrate and the half-saturation concentration of the light intensity K_I of the microorganism (in this case, *C. vulgaris*), was adapted from Tamiya et al. (1953) (Eq. (7a)). To account for the light absorption of the growing algae that leads to a decline in the incident light intensity during cultivation, the equation for average light from Jayaraman and Rhinehart (2015) was adapted for the shake flask setting. The depth D was defined as the average height of liquid in the shaken flasks, k_a indicates algal-turbidity, and the incident light I_B is calculated from the light sources light intensity I_s and the light duration chosen per day, L (Eqs. (7b) and (7c)).

The entire process model is defined through the following equations: balances expressed through ordinary differential equations in Eq. (6a) and (6b), growth rate in Eq. (7a), and average light intensity in Eq. (7b) and Eq. (7c).

Differential equations:

$$\frac{dX}{dt} = \left(\mu - \mu_D - \frac{F_M}{V}\right) \cdot X \tag{6a}$$

$$\frac{dV}{dt} = F_M - F_S \tag{6b}$$

Growth rate, light attenuation and duration:

$$\mu = \mu_{max} \cdot \frac{I_{avg}}{K_I + I_{avg}} \tag{7a}$$

$$I_{avg} = \left(\frac{I_B}{\alpha \cdot D}\right) \cdot \left(1 - e^{-\alpha \cdot D}\right) \tag{7b}$$

with $\alpha = k_a \cdot X$

$$I_B = I_s \cdot \mathbb{1}_{\left\{t - 24 \cdot \lfloor \frac{t}{24} \rfloor < L\right\}}(t) \tag{7c}$$

with indicator function $\mathbb{1}_{\left\{t - 24 \cdot \lfloor \frac{t}{24} \rfloor < L\right\}}$

The indicator function accounts for the light duration L and adopts the value 1 if the condition given in brackets holds, (here if $t - 24 \cdot \lfloor \frac{t}{24} \rfloor < L$), the light is switched on, otherwise it has a value of 0 when the light is switched off.

3.1.3. Modified model (Model 2) for C. vulgaris (CSB)

After the first mDoE cycle, the process model for *C. vulgaris* (Model 1) was modified to Model 2 and applied in the second cycle of mDoE.

In Model 2, an equation accounting for nitrate depletion was added and the radiation model was thoroughly revised. The model and its characterization for cultivating *C. vulgaris* in shake flasks with lighting from below have been described in detail in Kuhfuß et al. (2022) and are briefly explained below.

The concentration of nitrate c_N was considered because it is one of the primary nutrients required for the growth of microalgae (Andersen, 2005). The effects of nitrate concentration were integrated into the differential equation for biomass concentration (Eq. (9a)), and the nitrate uptake is expressed through Eq. (9b). The equation for the volume change (Eq. (9c)) was not altered.

Additional exploration of incident light inside the flasks during cultivation led to altered equations for light attenuation, on the basis of Cornet et al. (1997) and similarly to the model of CSA (Ifrim et al., 2014); in Model 2, Eq. (7b) and Eq. (7c) are replaced by Eq. (10).

Accordingly, some parameters change: D is replaced by z ($z \in [0, h]$), whereas h is defined as the maximum height of liquid inside the flasks for the path length of light in the flasks. Light attenuation is calculated with the Lambert–Beer equation, introducing four new parameters: the mass absorption coefficient E_a, mass scattering coefficient E_s, back scattering fraction b and ratio of spherical and hemispherical light per biomass concentration and height ε, as defined in Cornet et al. (1997). Consequently, α also has a new definition as the linear scattering modulus (Cornet et al., 1997).

I_s in Model 1 (Section 3.1.2), which was defined as the light intensity of the light source, is converted into the incident light

intensity I_0 before further calculation of the average light intensity I_{avg}. This alteration takes into account that a substantial portion of the light is lost on its way from the light source through the glass, owing to refraction and scattering, before passing through the medium ($z = 0$). I_0 can be calculated from I_s through the following equation (derived from a second degree polynomial regression based on light measurements):

$$I_0 = 6.92 + 0.436 \cdot I_s - 8.1 \cdot 10^{-5} \cdot I_s^2 \tag{8}$$

The full equations of Model 2 are as follows:

$$\frac{dX}{dt} = \left(\mu_{max} \cdot \frac{I_{avg}}{K_I + I_{avg}} \cdot \frac{c_N}{K_N + c_N}\right) \cdot X - \mu_D \cdot X - \frac{F_M}{V} \cdot X \tag{9a}$$

$$\frac{dc_N}{dt} = -Y_{N/X} \cdot \left(\mu_{max} \cdot \frac{I_{avg}}{K_I + I_{avg}} \cdot \frac{c_N}{K_N + c_N}\right) \cdot X - \frac{F_M \cdot c_N}{V} + \frac{F_M \cdot c_{N,Feed}}{V} \tag{9b}$$

$$\frac{dV}{dt} = F_M - F_S \tag{9c}$$

with

$$I_{avg}(t) = I_0 \cdot \frac{1}{\varepsilon X h} \cdot \left(1 - e^{-\varepsilon X h}\right) \cdot \mathbb{1}_{\left\{t - 24 \cdot \lfloor \frac{t}{24} \rfloor < L\right\}}(t) \tag{10}$$

with $\varepsilon = \frac{(1+\alpha)}{2\alpha} \cdot E_a$ for $\alpha = \sqrt{\frac{E_a}{E_a + 2bE_s}}$ and indicator function $\mathbb{1}_{\left\{t - 24 \cdot \lfloor \frac{t}{24} \rfloor < L\right\}}$, as in Model 1 in Eq. (7c).

$c_{N,Feed}$ is the nitrate concentration of the added feed, q_N is the depletion rate and $Y_{N/X}$ is a constant model parameter describing the ratio of the maximum nitrate uptake rate and maximum specific growth rate. K_N is the Monod kinetic constant for nitrate.

3.2. mDoE-toolbox

A model-assisted experimental design method, implemented in the software tool "mDoE-toolbox" (Möller et al., 2019), was applied in this study. With mDoE-toolbox, mathematical process models are used to describe the expected process variability (based on measurement errors), which is further used to plan and evaluate DoE designs computationally. This concept was previously introduced in Möller et al. (2019, 2020) and applied in Moser et al. (2021), and is briefly summarized below. As shown in Fig. 2, the objective of the study (i.e., maximization of biomass concentration) is defined in the beginning and the bioprocess is mathematically modeled on the basis of the available process understanding (e.g., literature data and experience).

The process variability based on the measurement errors is derived through Monte Carlo (MC) sampling (Box II). Therefore, the expected variability of each measured variable (e.g., biomass concentration and substrate concentration) is estimated. A DoE design is defined and the experimental factor combinations are planned with individual boundary values. Kuchemüller et al. (2020) have provided a review of various DoE designs and a selection scheme for their definition. Each recommended factor combination from the planned DoE is simulated multiple times with the mathematical process model and the time courses of the state variables are derived. The average expected response (e.g., average maximal biomass concentration) and its variability (differences in MC simulations) are calculated from the simulations. Then each defined factor combination is evaluated computationally (Box V), response surface plots are generated for visual assessment and only experiments with the desired outcome are recommended to be performed. This process enables risk-based decision-making for each planned experiment with respect to its simulated average and its expected variability, to simultaneously maximize the outcomes and minimize variability. If the comparison of simulated and experimentally derived response data shows that the applied model does not fit well, the model must be improved by using the gained process knowledge. Then another mDoE cycle is performed with the improved model, as described in Fig. 2 (dashed line).

3.2.1. Definition of design space

D. pseudocommunis in PBR (CSA)

A D-optimal design comprising 20 design points was planned for two factors. In CSA, the experimental factors incident light intensity I_0 and pH were considered; defining a lower and higher bound was necessary to plan the experimental settings. The lower and upper bounds for I_0 and pH were defined respectively, as:

$100\ \mu mol\,m^{-2}s^{-1} \leqslant I_0 \leqslant 800\ \mu mol\,m^{-2}s^{-1}$ and $6 \leqslant pH \leqslant 8$.

C. vulgaris in shake flasks (CSB)

In case study CSB the factors of incident light intensity I_0 and light duration per day L were selected as experimental factors. The lighting tablet enabled regulation of lighting between 300 $\mu mol\ m^{-2}s^{-1}$ and 1200 $\mu mol\,m^{-2}s^{-1}$ by a time switch to provide a light duration ranging from 1 to 24 h per day. Therefore, the lower and upper bounds for the above described factors are given respectively, by

$1\ h \leqslant L \leqslant 24\ h$ and $300\ \mu mol\,m^{-2}s^{-1} \leqslant I_s \leqslant 1200\ \mu mol\,m^{-2}s^{-1}$.

3.2.2. MC-based uncertainty quantification for both case studies

Parametric uncertainty was determined on the basis of the assumption of independent normally distributed measurement errors by using Monte Carlo (MC) sampling. The relative standard deviation (measurement uncertainty) was defined as 10% of the corresponding value for biomass concentration in CS A and for biomass and nitrate concentrations in CS B.

Then the model's parametric uncertainty was derived according to the experimental uncertainty by using multiple parameterization runs (MC simulations). Because of the computational power, 100 parameter estimation runs were performed in both case studies. Model parameters were adapted by minimizing the weighted squared differences between measured and simulated values with the Nelder-Mead simplex algorithm. To evaluate the adapted model (according to adapted model parameters), the coefficient of determination R^2 was used. This coefficient includes the ratio of the squared sum of differences between simulated $y_{s,i}$ and experimental data y_i, for $i = 1, \ldots, n$, and the sum of squared differences between experimental data and their mean $\bar{y}$:

$$R^2 = 1 - \frac{\sum_{i=1}^{n} \left(y_i - y_{s,i}\right)^2}{\sum_{i=1}^{n} \left(y_i - \bar{y}\right)^2} \tag{11}$$

R^2 has values between negative infinity and 1. Values near 1 indicate high agreement between the experimental and simulated data (Spiess and Neumeyer, 2010).

3.2.3. MC-based simulation of planned experiments and computational evaluation of experimental design for both case studies

The experiments proposed by the DoE (Section 3.2.1) were simulated with a corresponding mathematical model representing the underlying process (Sections 3.1.1 and 3.1.2.) To consider the propagated experimental variability, we performed MC simulations based on the determined parametric uncertainty as described in Section 3.2.2. Parameter values were sampled from a Latin hypercube space of the empirical parameter distribution by using the R-Package "lhs" (V1.0.2). In both case studies, 100 MC simulations were performed. For each simulated state variable, the 10% and 90% -quantiles of the obtained samples were computed to define 80% prediction intervals. To determine the accuracy between predicted and experimental biomass concentration values, the percentage error was calculated. The percentage error describes the percentage deviation between the simulated mean and the experimental value in relation to the experimental value, averaged over all values.

For evaluation of the experimental plan, the response values of the MC simulation for the maximum biomass concentration of cultivation were defined and calculated. Information on the expected response

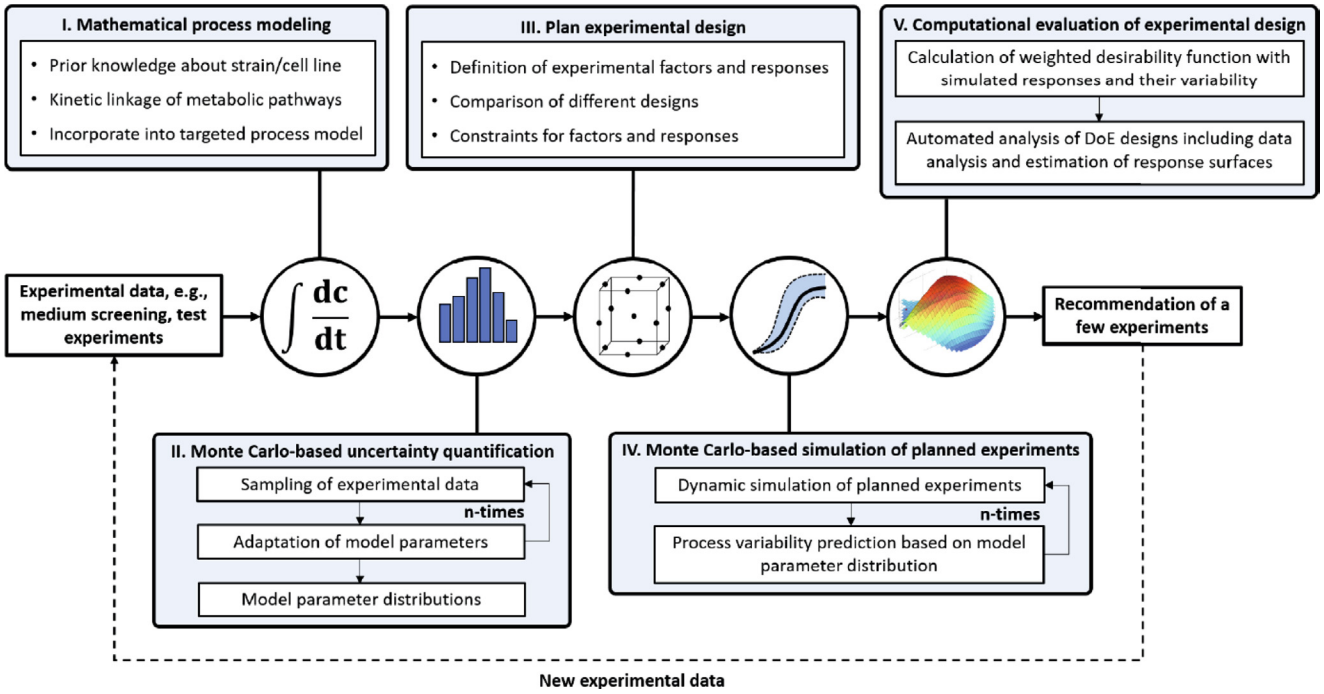

Fig. 2. Structural workflow of mDoE-toolbox consisting of the combination of mathematical process models and classical DoE under the consideration of model parametric uncertainty based on experimental variability, from Moser et al. (2021).

and the corresponding degree of uncertainty were embedded within proper desirability functions. To enable comparison, the expected response and the corresponding measure of uncertainty were scaled between 0 and 1. The desirability function D_{main} assigns the scaled expected response to each design point (factor combination) and the desirability function $D_{\Delta\text{percentile}}$ contains the scaled inverse of the width of the corresponding 80%-prediction interval. The inverse is taken because a low degree of uncertainty is desired which is consistent with a high inverse uncertainty value. Therefore, high values (close to 1) are desired for both, D_{main} and $D_{\Delta\text{percentile}}$. The desirability function D combines both desirability functions, assigning the weighted sum of D_{main} and $D_{\Delta\text{percentile}}$ to each design point, following

$$D = \frac{D_{\text{main}} + w \cdot D_{\Delta\text{percentile}}}{1 + w}. \tag{12}$$

Hence, maximizing D corresponds to the goal of maximizing the expected response while minimizing the corresponding uncertainty.

In this work, a weighting of $w = 0.4$ was applied to give more weight to the maximization of the expected response than to the minimization of uncertainty. Setting $w = 0.4$ leads to:

$$D = \frac{1}{1+w} \cdot D_{\text{main}} + \frac{w}{1+w} \cdot D_{\Delta\text{percentile}} \tag{13}$$

$$= \tfrac{1}{1.4} \cdot D_{\text{main}} + \tfrac{0.4}{1.4} \cdot D_{\Delta\text{percentile}}$$
$$= 0.71 \cdot D_{\text{main}} + 0.29 \cdot D_{\Delta\text{percentile}}.$$

Thus, the contribution of D_{main} is approximately 2.5 times higher than the contribution of $D_{\Delta\text{percentile}}$ to the desirability D.

4. Results and Discussion

The mDoE-toolbox was tested in the design of two microalgae processes. For the first process, CSA, a batch process for the strain *Desmodesmus pseudocommunis* (*D. pseudocommunis*) cultivated in a PBR was designed; for the second process, CSB, a batch process for the strain *Chlorella vulgaris* (*C. vulgaris*) cultivated in shake flasks was chosen.

In both case studies, the aim was to maximize the biomass concentration according to the experimental factors light intensity and pH (CSA), and light intensity and light duration per day (CSB). In CSA, a well established model was already available for the corresponding experimental setup.

The second case study, CSB, investigated whether mDoE-toolbox could also be used if no validated model was available in advance. For the use of mDoE, a simple mathematical model from the literature was used for the shake flask scenario. With this first model, a first cycle of mDoE was performed and the factor combination with the highest yield was identified. The use of mDoE provided the process understanding required to improve the model after the first mDoE cycle. Then the revised model was applied in a second mDoE cycle to investigate whether a better adapted process model might lead to different mDoE results than the simple model. The second mDoE cycle led to similar recommended factor combinations as the first. Thus, having an established model is not absolutely necessary to use mDoE successfully.

4.1. Application of mDoE-toolbox in the design of a microalgae process using D. pseudocommunis (CSA)

In this case study, the goal was to identify the optimal combination of two investigated factors, pH and light intensity I_0, leading to a maximum biomass growth rate of the microalgae *D. pseudocommunis*, cultivated in a PBR. The pH is a key factor for the photosynthetic growth of microalgae, being a result of the chemicals in the culture medium and the CO_2 sparging (Pegallapati and Nirmalakhandan, 2012). For *D. pseudocommunis* the optimal pH was assumed to be at 6.5. Although the pH is a dependent variable, as demonstrated in Ifrim et al. (2014) (CO_2 gas is the independent variable on the CO_2 - pH control channel), it was modeled here as an independent variable because it can be kept constant throughout the experiments to simplify the model. The importance of pH is even greater when it is controlled by CO_2 gas sparging, because the dissolved gas is the main carbon source of the photosynthetic microalgae.

The incident light intensity, in contrast, is an independent variable that can be set manually at a desired value. The incident light intensity is indispensable for photosynthesis, but it can also be inhibitory at higher values. It was anticipated that a kinetic growth equation for the specific growth rate, μ, would be a function of light and pH (closely related to the total inorganic carbon in this system). The factors I_0 and pH describe the specific growth rate of microalgae as a concave unimodal function (Eq. (2)). The optimal set of factors can thus be identified from a response surface.

4.1.1. Parameter estimation and MC-based uncertainty quantification

As shown in Fig. 2, Box II, the model parameters E_a, μ_{max}, μ_D and I_{opt} of the PBR model (Section 3.1.1) and and their distributions were identified by parameter estimation and MC sampling as described in Section 3.2.2, on the basis of the first data set for biomass concentration. The distributions of the four estimated parameters can be found in the Appendix (Fig. A1). The experiment was performed in batch mode at $I_0 = 400\ \mu mol\, m^{-2} s^{-1}$ and pH = 6.5, (Section 2.1).

The experimental biomass concentration values (dots) and the MC-based simulations (solid line) including 10% and 90% -quantiles (dashed lines) are shown in Fig. 3.

The experiment lasted approximately 6.5 days and achieved a biomass concentration of 2.8 $g L^{-1}$ after 152 h of cultivation time. Therefore, the volumetric growth rate was 0.184 $g L^{-1} h^{-1}$. The model parameters could be adjusted well so that the simulation fits the experimental values with an R^2 of 0.97.

4.1.2. Computational evaluation of experimental design

After identifying the parameter values and based on the defined experimental factors and their boundaries, we designed experiments with mDoE-toolbox (Box III in Fig. 2). A total of 20 experiments was suggested and distributed in the two-dimensional design space, and a D-optimal experimental design with the previously defined boundaries was applied, as described in Section 3.2.1. These experiments were simulated MC-based and with the growth model described in Section 3.1.1. Then the desirability D was calculated and the response surface was predicted, as outlined in Fig. 2 Box V. The desirability surface illustrated in Fig. 4 showed a maximum D, indicating that the highest biomass concentration of *D. pseudocommunis*, was expected for pH $\leqslant$ 7 and $I_0 \geqslant 400\ \mu mol\ m^{-2} s^{-1}$.

For pH values above 7.5 and a light intensity of $I_0 < 400\ \mu mol\, m^{-2} s^{-1}$, the obtained values of D were low ($D < 0.5$). Therefore, for lower light intensity values and higher pH, the expected biomass concentration of *D. pseudocommunis* would be much lower than the maximum achievable biomass.

4.1.3. Performed experiments

On the basis of the outcomes of the MC simulations and the evaluation of the response surface in Fig. 4, experiments in regions with a high desirability $D \geqslant 0.5$ were identified. The first recommended experiment, #2 with pH = 6.5 and $I_0 = 602\ \mu mol\ m^{-2} s^{-1}$, was performed as well as another experiment with high desirability, experiment #3, with pH = 7 and $I_0 = 795\ \mu mol\ m^{-2} s^{-1}$. MC simulations including lower bounds (10%-quantiles) and upper bounds (90%-quantiles) and experimental data are depicted in Fig. 5.

In the comparison of simulated and experimental values, an R^2 of 0.93 and 0.8 was achieved for the recommended experiments #2 and #3, respectively. To compare the three batches, the volumetric growth rates were calculated. The obtained results were: 0.0184 $g L^{-1} h^{-1}$ for #1, 0.026 $g L^{-1} h^{-1}$ for #2 and 0.018 $g L^{-1} h^{-1}$ for #3. Batch #2 with the factor combination pH = 6.5 and $I_0 = 602\ \mu mol\, m^{-2} s^{-1}$ led to the highest volumetric growth rate.

This result was consistent with the outcome of the mDoE (response surface in Fig. 4). The highest D-value concerning maximum biomass concentration was obtained in the region of pH = 6 to 6.5 and light intensity of 600 $\mu mol\, m^{-2} s^{-1}$.

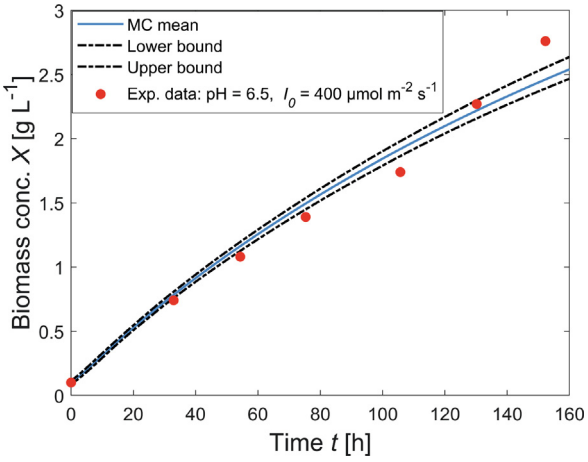

Fig. 3. Simulated and experimental biomass concentrations after parameter estimation (sample size 100) including 10% and 90% -quantiles for *D. pseudocommunis*.

In all three batches, the same amounts of nutrients were added into the culture medium. Because the pH was dependent on the bicarbonate buffer, (the pH of the culture medium without bicarbonate was approximately 5), the end of the batch coincided with the depletion of the bicarbonate. When the buffer was depleted, the pH could no longer be controlled, because the controller decreased the input CO_2 gas to zero to prevent the decrease in the pH. When the input CO_2 gas was decreased, the dissolved CO_2 also decreased, and the microalgae stopped growing. The dissolved CO_2 intake was thus proportional to the growth rate.

Fig. 6 shows the experimental data acquired from the sensors (i.e., dissolved CO_2, dissolved O_2, input CO_2 gas, pH and temperature) during the photosynthetic growth of microalgae cultivated at pH = 6.5, i.e., the two batches with the highest growth rates.

The depletion of bicarbonate is related with the concentration of dissolved CO_2, (Fig. 6, top left). Faster inorganic carbon intake results in a higher growth rate, as also confirmed by the biomass concentration measurements (batch #2, blue signal, had a higher growth rate than batch #1, red signal). The dynamics of the inorganic carbon in the system were even more complex, but the other data indicated the same conclusion. The input CO_2 gas in Fig. 6, top right, and the pH in Fig. 6, bottom left, (along with the previous discussed data for dissolved CO_2 and biomass concentration), indicated that a higher growth rate was associated with a lower CO_2 gas flow to regulate the same pH = 6.5. This result occurred because the system required less CO_2 to compensate for the pH-increase given by the remaining bicarbonate (blue signals point toward a faster inorganic carbon intake and hence a higher growth rate). The dissolved O_2 (Fig. 6, top center) was not associated with the inorganic carbon system, but it served as an excellent growth indicator. At the end of each batch the dissolved O_2 abruptly decreased thus indicating the end of the batch, associated with the depletion of the bicarbonate.

The experiment with the lowest growth rate, #3, was maintained at a non-optimal pH = 7, at which the photosynthetic production of O_2 was very low (close to zero) and thus the data acquired by the dissolved O_2-probe were not relevant (not shown). The data acquired from sensors could not be compared in the same manner as above (i.e., #1 with #2) when the pH values differed because the molecular and ionic species of the total inorganic carbon are pH-dependent (the thermodynamic equilibrium shifts toward the dissolved CO_2 as the pH decreases). However, the biomass concentration data were comparable, and the volumetric growth rate could easily be determined.

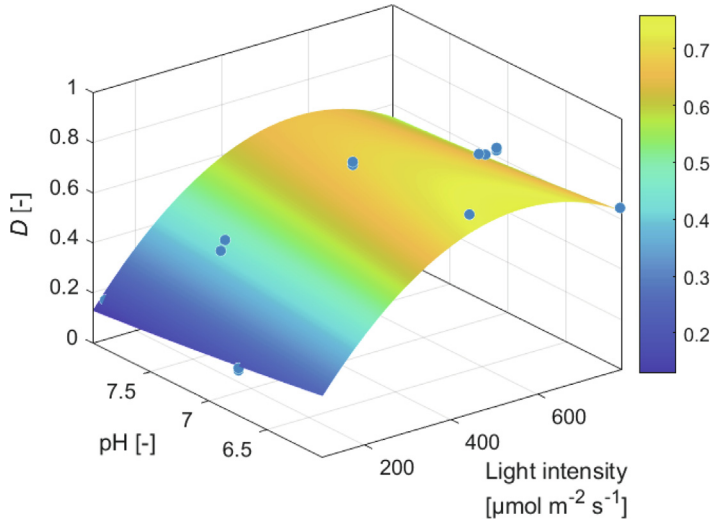

Fig. 4. 3D plot showing the desirability values D (dots) for various factor combinations and the corresponding response surface for the optimal biomass concentration of *D. pseudocommunis*.

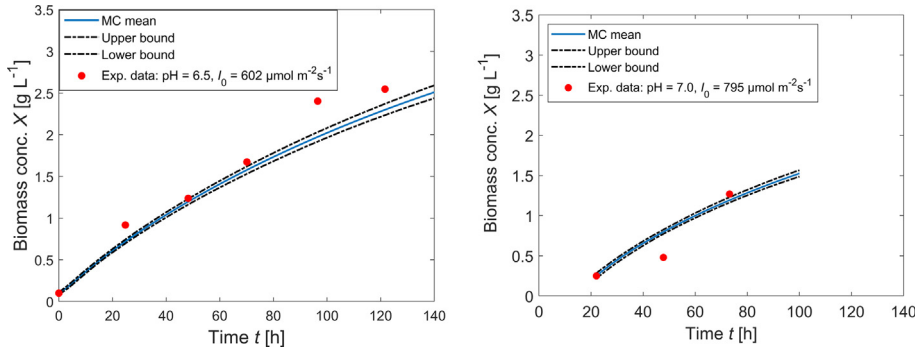

Fig. 5. Performed experiments recommended by mDoE-toolbox for *D. pseudocommunis*, exp. #2 (left, pH $= 6.5$ and $I_0 = 602$ µmol m^{-2} s^{-1}) and exp. #3 (right, pH $= 7$ and $I_0 = 795$ µmol m^{-2} s^{-1}), showing the MC mean (blue solid line), lower bounds (10%-quantiles) and upper bounds (90%-quantiles) and experimental data (red dots).

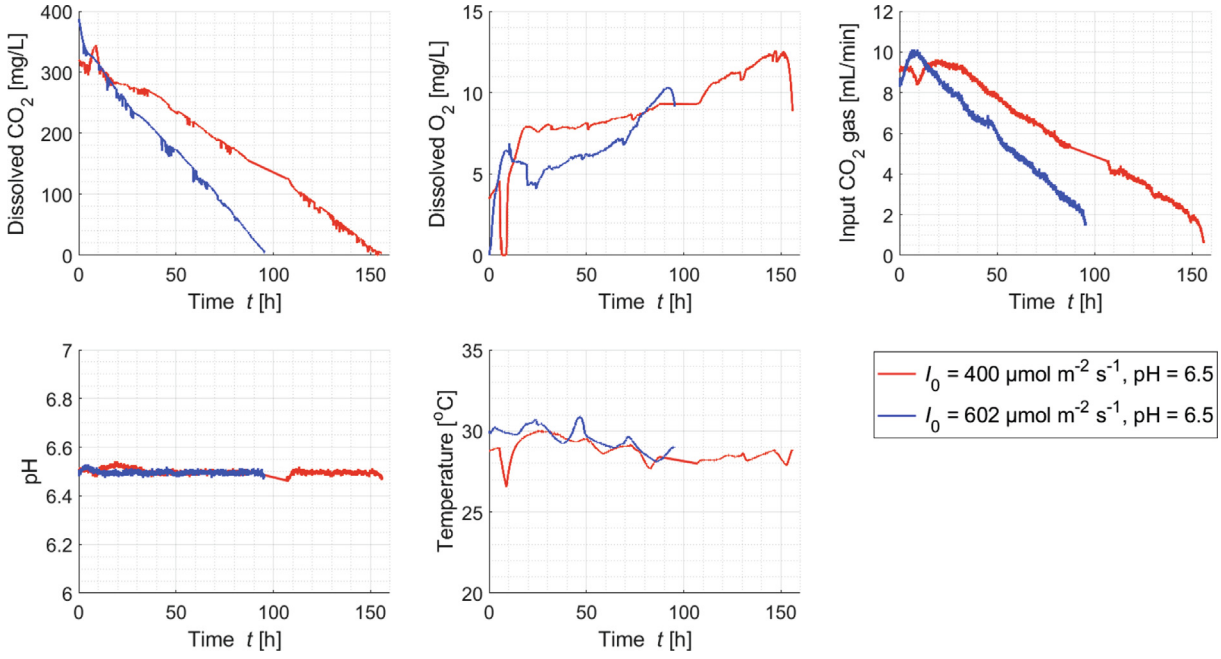

Fig. 6. Experimental data acquired from the 2 batches performed on the photobioreactor with *D. pseudocommunis*, red for experiment #1, blue for experiment #2.

In summary, in case study CS A, mDoE-toolbox was successfully applied to identify combinations of light intensity and pH leading to a higher biomass yield for *D. pseudocommunis* cultivated in a PBR, as compared with the results with application of the reference factor combination (#1). A sole experiment was sufficient to identify the experimental setting leading to a maximum biomass concentration, which was a combination of pH = 6.5 and $I_0 = 602$ μmol m^{-2} s^{-1}. Two further experiments were performed to verify the predicted biomass concentration for the recommended factor combinations and to confirm the calculated higher growth rate. Thus, the control of pH and light (for artificially lighted PBRs) led to higher volumetric growth rates: the volumetric growth rate of experiment #2 was more than twice the rates reported in the literature for *D. pseudocommunis* in batch cultivation (Zhang et al., 2019) and was even higher than those stated for a fed-batch cultivation (Del Rio-Chanona et al., 2019). Several *Scenedesmus ssp.*, from the same genus as *D. pseudocommunis*, have been found to achieve only one third of the volumetric growth rate of experiment #2, Gouveia and Oliveira (2009, 2020, 2011).

4.2. Application of mDoE-toolbox to the design of a C. vulgaris process (CS B, first cycle, initial model)

The second case study, CS B, investigated whether mDoE-toolbox could also be used, if no validated model is available in advance. To our knowledge, no mathematical model for the shake flask setting of *C. vulgaris* was available, so an appropriate model needed to be identified for the application of mDoE. The model from CS A was unsuitable because it describes a different species of algae and it is based on the pH, which cannot be adjusted in this experimental arrangement, in which the pH is kept in the desired range by means of buffers. In addition, the light equation in CS A contains an inhibition term, whereas Monod kinetics is common for *Chlorella*, Filali et al. (2011, 2013). For the mDoE application, a simple mathematical model was used for the shake flask scenario, on the basis of Monod kinetics combined with a Lambert–Beer radiation model from the literature (Tamiya et al., 1953; Jayaraman and Rhinehart, 2015), as described in Section 3.1.2.

4.2.1. Parameter estimation and MC-based uncertainty quantification

As illustrated in Fig. 2, Box II, model parameters and parametric uncertainties are determined in this step by using parameter estimation and MC sampling (Section 3.2.2). The data applied in this step were gathered from the experiments described in Section 2.2. These were performed at 300 (experiment #1), 750 (experiment #2) and 1200 μmol m^{-2} s^{-1} (experiment #3), each with 12 h of daily lighting. The model as depicted in Section 3.1.2 contains four model parameters. Three of the parameters, k_a, K_I, and μ_{max}, were estimated, whereas μ_D was set to 0.0018 h^{-1} because of its minor influence (in the literature values for μ_D range from 0 h^{-1} to 0.0056 h^{-1} for *C. vulgaris* (Concas et al., 2012; Lee et al., 2015). The distributions of the three estimated parameters are unimodal and can be found in the Appendix (Fig. A2). The maxima of the distributions are approximately 49 $L g^{-1} m^{-1}$ for k_a, 0.058 h^{-1} for μ_{max} and 125 μmol $m^{-2} s^{-1}$ for K_I. The estimated model parameters resulted in simulations that fit the experimental values with an R^2 of 0.84 (#1), 0.69 (#2) and 0.45 (#3). The applied model achieved better agreement between simulated and experimental data for lower light intensities (see Fig. 7).

4.2.2. Computational evaluation of experimental design

In a next step, a total of 20 experiments were designed by mDoE-toolbox on the basis of the defined factors, their boundaries and the chosen design (cf. Box III in Fig. 2). The experiments were located in the two-dimensional design space with the previously defined boundaries described in Section 3.2.1.

These experiments were simulated with Model 1 for *C. vulgaris* and the adapted model parameters, as explained in Section 4.2.1, in combination with MC sampling. The obtained distributions for the maximum biomass concentration (means and quantiles of prediction bands) were used to calculate the desirability values D_i for each factor combination i (Box V in Fig. 2, and Section 3.2.3). Then a response surface was estimated for D. Desirability values and the corresponding response surfaces are shown in Fig. 8 (left). The most appropriate factor combination, i.e., that leading to the highest D (0.74), was obtained when the light intensity and duration were equal to 1200 μmol $m^{-2} s^{-1}$ and 23 h, respectively. The designed experiments located in the lower part of the response surface plot for the response surfaces in Fig. 8 (left) achieved low desirability ($D \leqslant 0.5$). Consequently, these experiments were not necessary to perform.

In contrast, the designed experiments located in the upper part of the response surface plot with $I_s \geqslant 750$ and $L \geqslant 12$ promised to yield desired results ($D \geqslant 0.5$). Thus, the experimental design space could be reduced to the experimental settings located in the upper part. As outlined in Box III in Fig. 2, the new lower and upper bounds for the light intensity and duration were reduced to: $12\,h \leqslant L \leqslant 24\,h$ and $750\,\mu mol\,m^{-2}s^{-1} \leqslant I_s \leqslant 1200\,\mu mol\,m^{-2}s^{-1}$. Again, a total of 20 experiments were designed for the two-dimensional experimental design space. The designed experiments were analyzed as described in Section 3.2.3. MC simulations were performed to compute the maximum biomass concentration (mean and quantiles) as well as the corresponding desirability value D_i for each experimental setting i and the corresponding response surface, as illustrated in Fig. 8, right.

According to Fig. 8, setting the light duration to $L \geqslant 18$ h and the light intensity to $I_s \geqslant 750\,\mu mol\,m^{-2}s^{-1}$ resulted in higher desirability ($D \geqslant 0.5$). Thus, the experiments located in the upper right corner of the experimental space in Fig. 8 (right) were assumed to provide high biomass concentrations of *C. vulgaris* within the defined experimental design space.

4.2.3. Performed experiments

The experiments with the highest D-values were recommended by mDoE-toolbox. Three of the recommended experiments were selected to be performed and are presented in Table 1.

In Fig. 9 the experimental values of biomass concentration are compared with the simulated values, including the parametric 10% and 90% uncertainty-based prediction bands. As expected and as predicted by the response surfaces, experiment #4 qualitatively achieved the highest biomass concentration with 5.7 $g L^{-1}$ after 165 h. The biomass densities achieved after a cultivation time of approximately 165 h are shown in Table 2. The mean value for four flasks from each performed experiment is shown and compared with the mean of 100 MC simulations from the model. The respective percentage error is also indicated. The comparison in Fig. 9 shows that the model provided correct simulations during the first 72 h in case of experiment #4 and #5 and the first 96 h in case of experiment #6. The model then overestimated the biomass growth with a percentage error as high as 240%. The maximum biomass concentration was overestimated in all three experiments with a percentage error of more than 100%. Taking into account all six performed experiments (three for parameter estimation and three recommended experiments), the conclusion was drawn that the applied model required an improvement regarding the effects of light (light intensity and light duration) on biomass growth, particularly with augmented concentrations of microalgae (density) in shake flask.

However, compared with other studies, experiments #4 and #6 led to similar or even higher maximum biomass concentrations. Some studies, in which *C. vulgaris* was cultivated under various experimental conditions (concerning light and cultivation vessel), have reported biomass densities below 1 $g L^{-1}$ (Wong et al., 2016; Matos et al., 2015) or

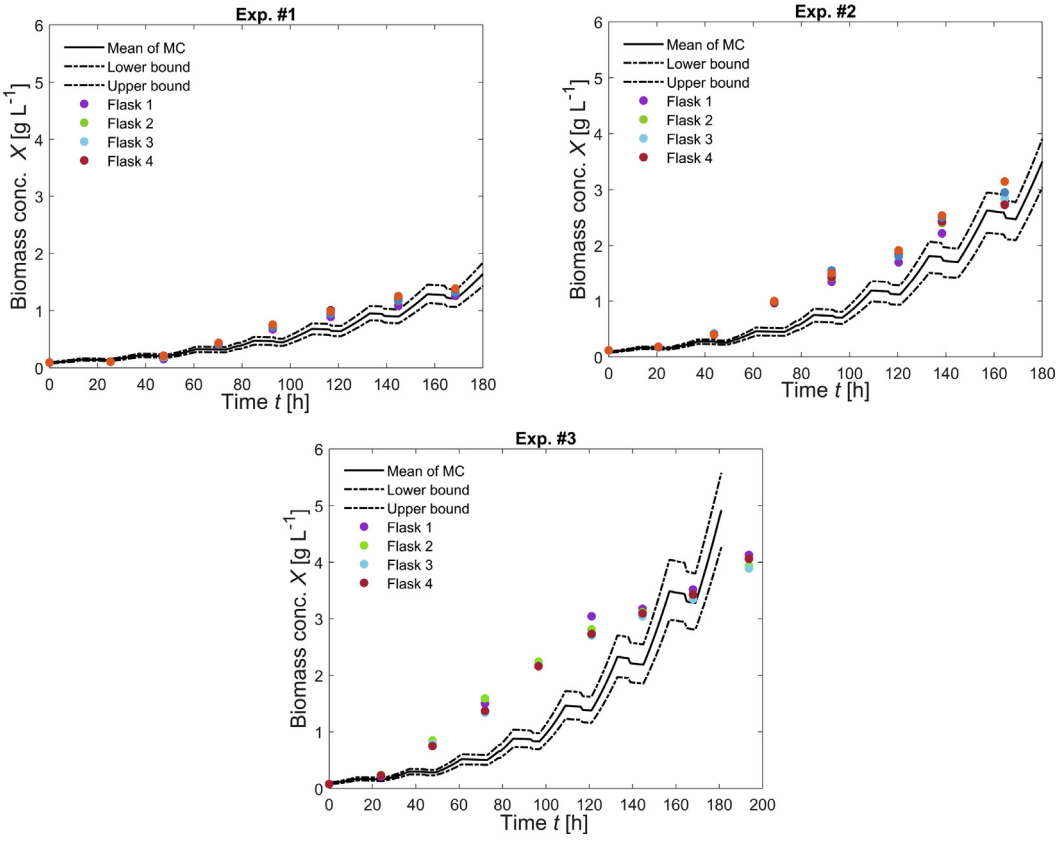

Fig. 7. Experimental and simulated values for biomass concentration after estimation of the model parameters k_a, μ_{max} and K_1 for *C. vulgaris* Model 1. Experiments were performed at 300 (experiment #1), 750 (experiment #2), and 1200 µmol m^{-2} s^{-1} (experiment #3), each under 12 h of daily lighting. The solid line depicts the mean of 100 simulations and the dashed lines represent the corresponding 10% and 90%-quantiles.

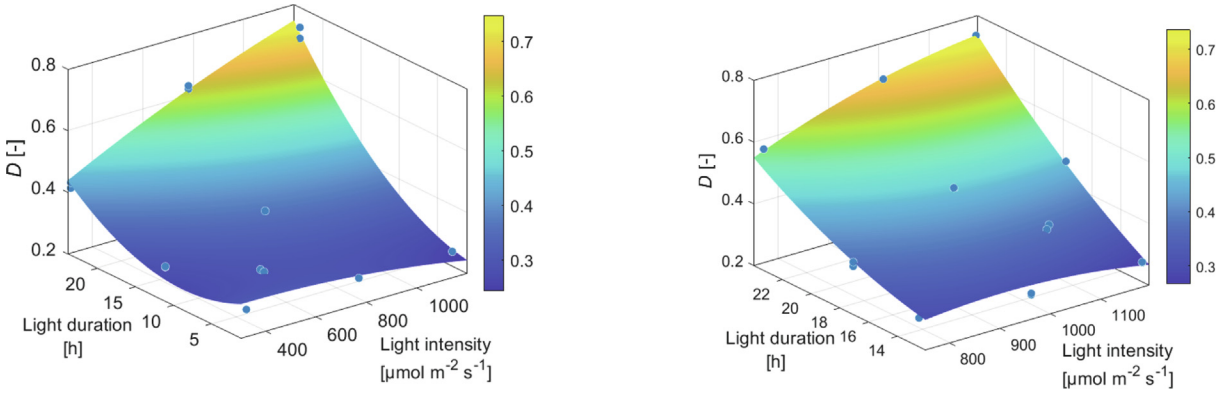

Fig. 8. Desirability values *D* (dots) for various factor combinations and the corresponding response surface for the optimal biomass concentration of *C. vulgaris* for the first iteration (before reduction of the design space, left) and for the second iteration with the reduced design space considering only the higher values of light duration and light intensity (right).

below 3 gL^{-1} (Mirzaie et al., 2016). Results comparable to those of this study have been presented in Morschett et al. (2017), which provides a comparison of three cultivation systems and has reported a biomass concentration of 5.5 gL^{-1} in shake flasks.

From the first round of experiments it was concluded that only three experiments were necessary to identify the factor combinations leading to high biomass concentrations. The experiments performed according to the recommendation of mDoE-toolbox confirmed that the factor combination with the highest *D* (experiment #3: 1200 µmol $m^{-2}s^{-1}$ light intensity with 12 h lighting) also resulted in very high biomass concentrations in the performed experiments, averaging 5.7 g L^{-1}. Another benefit was that the mDoE-method revealed where model improvements were necessary. Valuable process

Table 1
Factor combination (light duration *L* and light source intensity I_s) of the three *C. vulgaris* cultivation experiments out of 20, determined by mDoE-toolbox.

Experiment	Light duration *L* [h]	Light source intensity I_s [μmol $m^{-2}s^{-1}$]
#4	24	1200
#5	24	750
#6	21	859

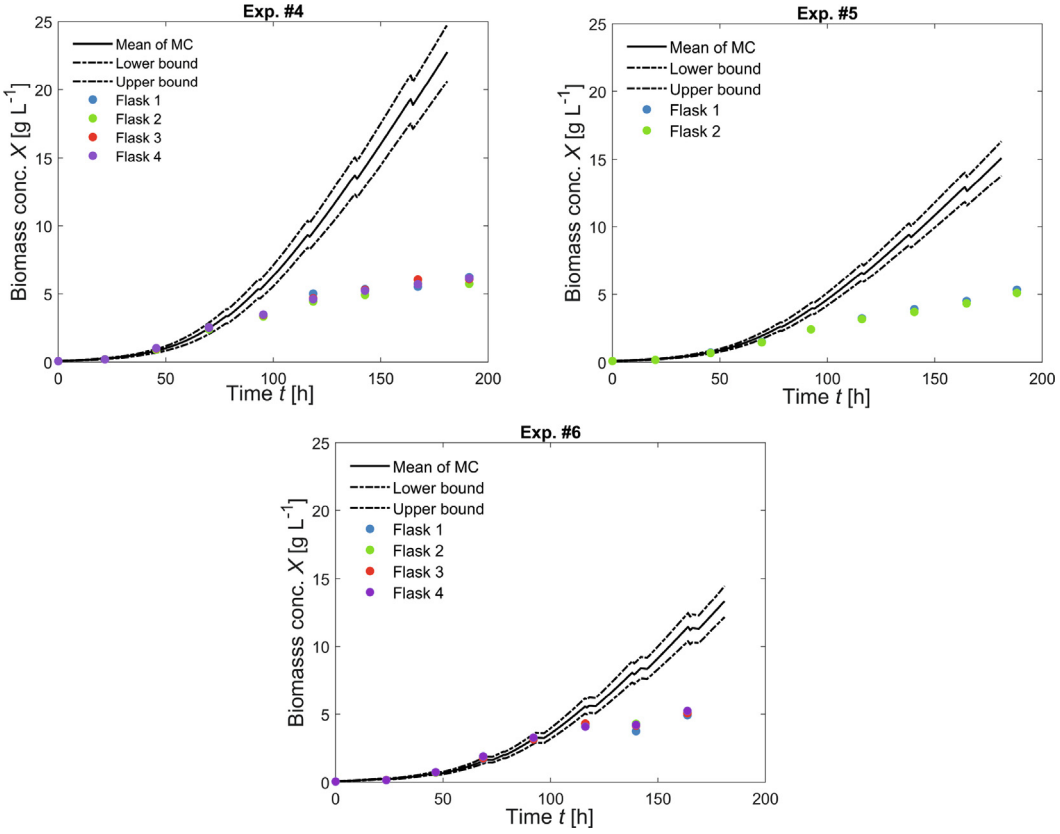

Fig. 9. Experimental data (dots) of the three performed cultivations at 1200 µmol $m^{-2}s^{-1}$ during 24 h (#4), 750 µmol $m^{-2}s^{-1}$ during 24 h (#5) and 859 µmol $m^{-2}s^{-1}$ during 21 h (#6) compared with the simulated data from the mDoE-toolbox for the biomass concentration. The solid line depicts the mean of 100 simulations and the dashed lines represent the corresponding 10% and 90% -quantiles.

Table 2
Experimental (X_{Exp}) and simulated values (X_{Sim}) of biomass concentration (conc.) X after approximately 165 h, for different combinations of light duration L and light source intensity I_s, together with the corresponding percentage error (Perc. error) using the initial model of *C. vulgaris* (Model 1).

Experiment	Light duration and intensity		Biomass conc. at approximately 165 h		Perc. error
	L [h]	I_s [µmol $m^{-2}s^{-1}$]	X_{Exp} [g L^{-1}]	X_{Sim} [g L^{-1}]	[%]
#4	24	1200	5.7	19.4	240
#5	24	750	4.4	12.6	186
#6	21	859	5.1	11.4	124

knowledge was generated, which could be used for model improvement and for a second mDoE cycle.

4.3. Application of mDoE (CSB, second cycle, re-adapted model)

The results of the first mDoE cycle showed that approximately from day 3 onward, Model 1 did not predict biomass concentration reliably. Model 1 probably does not provide a good description of the effects of light intensity on biomass growth or the average light intensity itself. In addition, another limiting factor might need to be considered. On the basis of these assumptions, the model equation describing the average light intensity was improved and nitrate was integrated into the model as a limiting factor.

A second mDoE cycle was performed on the basis of the improved model for *C. vulgaris* cultivation in shake flasks, as summarized in Section 3.1.3. A more detailed description and evaluation can be found in Kuhfuß et al. (2022). The outcomes of parameter estimation and evaluation of experimental design are presented in the following sections.

4.3.1. Parameter estimation and MC-based uncertainty quantification

Parameter estimation applying MC-based uncertainty quantification was performed according to the available data sets used in the first mDoE cycle (experiments #1 - #6, Table 1). Model parameters (Model 2 in Section 3.1.3) concerning local light intensity and nitrate uptake were identified in Kuhfuß et al. (2022) and were fixed in this work. The remaining three model parameters, the maximum growth rate μ_{max}, death rate μ_D and the half saturation constant of light K_I, were estimated by applying 100 parameter estimation runs to obtain representative distributions. In each run, two flasks for each factor combination were sampled randomly, and a normally distributed measurement uncertainty of 10% relative standard deviation was assumed. MC simulations and experimental values for biomass concentration are presented in Fig. 10.

The distribution of model parameters is illustrated in Fig. A3 in the Appendix. It can be seen that Model 2 achieved a high agreement between the simulated and experimental data for various light intensities and duration over the entire time span, not only during the first 72 h. One reason for this result may be that Model 2 contains an

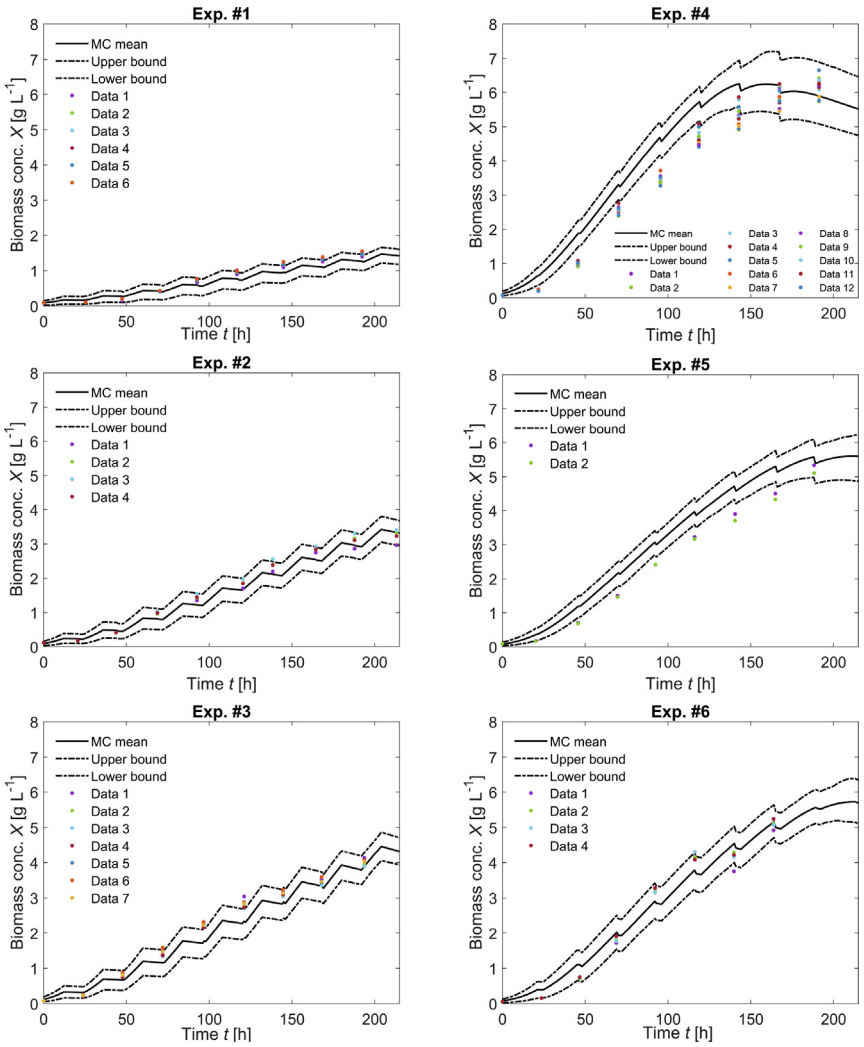

Fig. 10. Comparison of the experimental and the simulated biomass concentration data with the re-adapted model (Model 2) for experiments #1 (I_s = 300 µmol m^{-2}s^{-1}, 12 h), #2 (I_s = 750 µmol m^{-2}s^{-1}, 12 h), #3 (I_s = 1200 µmol m^{-2}s^{-1}, 12 h), #4 (I_s = 1200 µmol m^{-2}s^{-1}, 24 h), #5 (I_s = 750 µmol m^{-2}s^{-1}, 24 h) and #6 (I_s = 859 µmol m^{-2}s^{-1}, 21 h). The solid line depicts the mean of 100 simulations and the dashed lines represent the 10% and 90% -quantiles of the simulations. Light intensities and duration as in Table 3.

improved term for light absorption in shake flasks when the biomass concentration increases. Another reason may be that Model 2 considers the limiting effect of nitrate depletion (nitrate was not considered in Model 1 because it was assumed that sufficient nitrate would be available during the entire cultivation).

Table 3 lists the average coefficient of determination (R^2) and the average percentage error for all six factor combinations. An R^2 higher than 0.9 was found for all experiments except experiment #5 (R^2 = 0.83). Compared with the percentage error obtained for experiments #4, #5 and #6 using Model 1, a marked improvement was achieved (28% instead of 240%, 45% instead of 186% and 22% instead of 124%, as compared with values in Table 2).

4.3.2. Computational evaluation of experimental design

The same experimental factors, boundaries and settings as defined in the first cycle after reduction of the design space were also used in the second cycle. With MC simulations, the desirability D_i concerning maximum biomass concentration X_{max} was obtained for each experimental setting *i*. The obtained response surface in Fig. 11 was not exactly the same as that in Fig. 8, but high desirability values were obtained for combinations with high light duration and high light intensities and the maximum *D* was obtained for the experimental setting of 24 h light duration and 1200 µmol m^{-2}s^{-1}. Furthermore, the change in light duration led to a larger change in *D* (e.g., from 0.3 to 0.7 at 800 µmol m^{-2}s^{-1} or from 0.4 to 0.85 at 1200 µmol m^{-2}s^{-1}) than changing the light intensity within the defined boundaries (e.g., from 0.3 to 0.4 at 12 h light duration or 0.7 to 0.85 at 24 h light duration).

4.3.3. Performed experiments

In the second cycle of mDoE, the factor combination with the highest *D* was the same as that in the first mDoE cycle, a light intensity of 1200 µmol m^{-2}s^{-1} with 24 h light duration. To confirm the previous outcome (6 g L^{-1} maximum biomass concentration), the experiment was repeated (denoted by #7). The MC simulation (means, 10% and 90% -quantiles) based on parameter distributions determined in the second cycle and experimental values from 12 flasks is shown in Fig. 12.

An R^2 of 0.85 and a percentage error of 0.32% was achieved for the agreement between the measurements and predictions. In experiment #7, a maximum biomass concentration of 6.6 g L^{-1} on average (range: 5.4 to 8 g L^{-1}) was reached, and the initially identified optimal factor combination of I_s = 1200 µmol m^{-2}s^{-1} and 24 h was confirmed. As compared with that in the first experiment, #3, with lower light

Table 3
Goodness of fit scores: Coefficient of determination (R^2) and percentage error (Perc. error) for all six factor combinations of light duration L and light source intensity I_s for *C. vulgaris* after parameter estimation based on Model 2.

Experiment	Light duration	Light source intensity	Coeff. of det.	Percentage error
	L [h]	I_s [µmol m^{-2}s^{-1}]	R^2 [-]	[%]
# 1	12	300	0.94	21
# 2	12	750	0.97	14
# 3	12	1200	0.91	17
# 4	24	1200	0.96	28
# 5	24	750	0.83	45
# 6	21	859	0.97	22

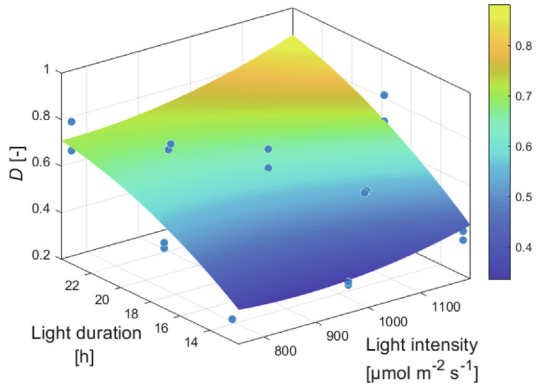

Fig. 11. Desirability values D (dots) for various factor combinations and the corresponding response surface for the maximum biomass concentration of *C. vulgaris* with Model 2 (second mDoE cycle).

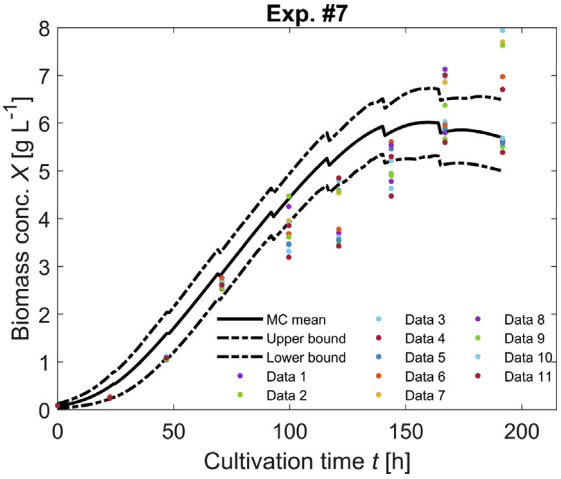

Fig. 12. Simulated and experimental biomass concentration values for the recommended experiment (1200 µmol m^{-2}s^{-1} with 24 h light duration), second mDoE cycle *C. vulgaris*. MC means (solid line), 10%- and 90%-quantiles of MC simulations (dashed lines) and experimental data (dots) from 12 shake flasks are shown.

duration (I_s = 1200 µmol m^{-2}s^{-1}, 12 h), the maximum biomass concentration doubled.

These biomass concentrations exceeded the biomass concentrations reported in the literature, wherein, for *C. vulgaris*, an average biomass concentration of 1.5 g L^{-1} after 9 days was indicated, and that for different *Chlorella ssp.* was between 0.45 g L^{-1} and 5.6 g L^{-1} (Griffiths et al., 2011). In other microalgae strains, maximum biomass concentrations below 3 g L^{-1} have been reported, e.g., for the microalgae *Haematococcus pluvialis* (Zhao et al., 2019; Zhang et al., 2016). In a continually lighted flat-plate bioreactor setting, a biomass concentration of 5.0 g L^{-1} after 4 days has been reported for cultivation of *Scenedesmus obtusiusculus* (Koller, 2017). In summary, in the first cycle of mDoE the experimental settings leading to a maximum biomass concentration, which were 1200 µmol m^{-2}s^{-1} light intensity with 24 h light duration, were determined with a minimum of experiments (300, 750 and 1200 µmol m^{-2}s^{-1}-light intensity with 12 h light duration), as compared with the 20 experiments proposed by the designed DoE. Moreover, valuable process knowledge was generated within the first mDoE cycle and could be used for model improvement and for a second mDoE cycle.

Three additional experiments were performed: 1200 µmol m^{-2}s^{-1} with 24 h light duration (#7), 750 µmol m^{-2}s^{-1} with 24 h light duration (#5) and 859 µmol m^{-2}s^{-1} with 21 h light duration (#6). These experiments were chosen from among the recommended experiments of the first mDoE cycle, to explore whether the biomass concentration values predicted by the response surface of mDoE could be confirmed. The mean values of the achieved biomass concentration in experiments #5 and #6 were similar (5.0 g L^{-1} and 4.8 g L^{-1}). A 12.5% shorter light duration in experiment #6 had a similar effect on growth as a 12.5% decrease in light intensity in experiment #5. These findings are in agreement with the predicted desirability values of mDoE-toolbox.

Notably, at the beginning of this case study, no well established model was available for the cultivation of *C. vulgaris* in shake flasks. However, the mDoE method was found to be sufficiently robust to identify the region of the factor combinations with high desirability values. The new data from the recommended experiments were compared with the output of the mathematical model, which indicated that improvement of the model structure was necessary. The critical process parameters were those concerning light attenuation over time. The successful application of the mDoE approach led to advanced process understanding and enabled the development of a convenient mechanistic model for phototrophic growth in the shake flask setting. In CSB the use of mDoE was a time-saving, cost-effective and useful method for the design of a microalgae bioprocess. The second mDoE cycle confirmed the findings from the first cycle regarding the experiment with the highest desirability. The results indicated that the number of experiments necessary for process development can be decreased with the mDoE-approach, even if an established model is not available.

5. Conclusion

The mDoE-method, introduced by Möller et al. (2019), was evaluated in the context of two microalgae processes. In the first case study (CSA), *D. pseudocommunis* was cultivated in a PBR; in the second case study (CSB), *C. vulgaris* was cultivated in shake flasks. In both applications of the mDoE-method, the aim was to identify the combination of

two experimental factors that led to a maximum biomass yield at the end of cultivation. The two experimental factors were light intensity and pH in CSA, and light intensity and light duration in CSB. In CSA, the factor combinations of pH and light intensity, which led to a higher biomass growth of *D. pseudocommunis* cultivated in a PBR, compared with the reference factor combination, were identified after one experiment. In that case, a previously validated model was available, and only one experiment was performed for model adaption. Two further experiments were performed to confirm the predicted biomass growth. The biomass growth rate was increased by 44% with respect to the first reference experiment.

In CSB, a challenging aspect was that no well-established model was available to model biomass growth under the applied experimental conditions. This case study indicated that mDoE can also be applied with a model still needing improvement. In the first mDoE cycle, a simple model based on Monod kinetics was applied, and the region within the experimental space that produced high biomass growth was identified with only three experiments. The identified factor combinations were consistent with the expected results and were confirmed with an improved mechanistic model in a second mDoE cycle. During the successful application of mDoE toolbox for bioprocess development, valuable process knowledge was gained regarding the interaction of critical process parameters.

Both case studies demonstrated the advantage of the presented mDoE-toolbox. With this method, in contrast to classical DoE, only very few experiments were necessary to identify improved factor combinations, in this case, maximum biomass growth. This process was enabled by the embedded knowledge-driven and risk-based approach of mDoE.

Declaration of Competing Interest

The authors declare that they have no known competing financial interests or personal relationships that could have appeared to influence the work reported in this paper.

Acknowledgements

The authors acknowledge funding from the German Federal Ministry of Education and Research (BMBF, grant 031B0577A-C).

Appendix A

Tables A.1,A.2,A.3,A.4
Figs. A1,A2,A3

Table A.1
Medium component suppliers for *C. vulgaris*.

Medium component	Supplier; Headquarters
KNO_3	VWR Chemicals/ VWR International GmbH; Darmstadt
NaCl	VWR Chemicals/ VWR International GmbH; Darmstadt
$NaH_2PO_4 \cdot 2\ H_2O$	Merck KGaA; Darmstadt
$Na_2HPO_4 \cdot 12\ H_2O$	Honeywell Riedel de Haën AG; Seelze
$MgSO_4 \cdot 7\ H_2O$	Carl Roth GmbH + Co KG; Karlsruhe
$CaCl_2 \cdot 2\ H_2O$	VWR Chemicals/ VWR International GmbH; Darmstadt
$FeSO_4 \cdot 7\ H_2O$	Merck KGaA; Darmstadt
$MnCl_2 \cdot 4\ H_2O$	Merck KGaA; Darmstadt
H_3BO_3	Carl Roth GmbH + Co KG; Karlsruhe
$ZnSO_4 \cdot 7\ H_2O$	Honeywell Riedel de Haën AG; Seelze
$(NH_4)_6MO_7O_{24} \cdot 4\ H_2O$	Merck KgaA; Darmstadt
EDTA-Na_2	VWR Chemicals/ VWR International GmbH; Darmstadt
H_2O (bidistilled)	Produced locally

Table A.2
Full list of model parameters and units of the models for *D. pseudocommunis* (CSA) and *C. vulgaris* (CSB).

Parameter	Definition	Unit	Model
X	Biomass concentration	$g\,L^{-1}$	CSA + CSB
t	Time	h	CSA + CSB
μ	Specific growth rate	h^{-1}	CSA + CSB
μ_D	Specific death rate	h^{-1}	CSA + CSB
μ_{max}	Maximum specific growth rate	h^{-1}	CSA + CSB
F_M	Medium feed rate	$L\,h^{-1}$	CSB
F_S	Sample rate	$L\,h^{-1}$	CSB
V	Volume	L	CSB
I_B	Incident light intensity (Model 1)	$\mu mol\,m^{-2}s^{-1}$	CSB
I_{avg}	Average light intensity	$\mu mol\,m^{-2}s^{-1}$	CSB
I_s	Light intensity (light source)	$\mu mol\,m^{-2}s^{-1}$	CSB
I_0	Incident light intensity (Model 2)	$\mu mol\,m^{-2}s^{-1}$	CSB
$I(z)$	Local light intensity	$\mu mol\,m^{-2}s^{-1}$	CSA
I_{min}	Minimum local light intensity	$\mu mol\,m^{-2}s^{-1}$	CSA
I_{max}	Maximum local light intensity	$\mu mol\,m^{-2}s^{-1}$	CSA
I_{opt}	Optimal local light intensity	$\mu mol\,m^{-2}s^{-1}$	CSA
ε	Ratio of spherical to hemispherical light per biomass concentration and height	$m^2\,kg^{-1}$	CSA + CSB
α	Total extinction coefficient or linear scattering modulus	m^{-1} or -	CSA + CSB
k_a	Algal turbidity	$L\,g^{-1}\,m^{-1}$	CSB
k_n	Non-algal turbidity	m^{-1}	CSB
z or D	Depth (system)	m	CSA + CSB
h	Height	m	CSB
K_I	Light associated half-saturation concentration	$\mu mol\,m^{-2}s^{-1}$	CSA + CSB
K_N	Uptake rate associated Monod kinetic constant	$g\,L^{-1}$	CS B
E_a	Mass absorption coefficient	$m^2\,kg^{-1}$	CSA + CSB
E_s	Mass scattering coefficient	$m^2\,kg^{-1}$	CSA + CSB
b	Back scattering fraction	-	CSA + CSB
L	Depth of the reactor	m	CSA
L	Light duration per day	h	CSB
q_N	Nitrate uptake rate	$g_{nitrate}\,g_{biomass}^{-1}\,h^{-1}$	CSB
q_{Nmax}	Maximum nitrate uptake rate	$g_{nitrate}\,g_{biomass}^{-1}\,h^{-1}$	CSB
c_N	Nitrate concentration	$g\,L^{-1}$	CSB
$c_{N,Feed}$	Nitrate concentration feed	$g\,L^{-1}$	CSB
$Y_{N/X}$	Ratio of max. nitrate uptake rate and max. specific growth rate	$g_{nitrate}g_{biomass}^{-1}$	CS B
pH	pH value (system)	-	CSA
pH_{min}	Minimum pH value	-	CSA
pH_{max}	Maximum pH value	-	CSA
pH_{opt}	Optimal pH value	-	CSA

Table A.3
List of abbreviations.

CSA or CSB	first (A) or second (B) case study
C. vulgaris	*Chlorella vulgaris*
DoE	Design of Experiments
MC	Monte Carlo
mDoE	Model-assisted Design of Experiments
PBR	photobioreactor
SAG	Collection of Algae Cultures of the University of Göttingen
D. pseudocommunis	*Desmodesmus pseudocommunis*
V/V	volume per volume

Table A.4
List of symbols.

Symbol	Meaning	Unit
α	Total extinction coefficient or linear scattering modulus	m^{-1} or -
ε	Ratio of spherical to hemispherical light per biomass concentration and height	$m^2 kg^{-1}$
λ	Wavelength	nm
μ	Specific growth rate	h^{-1}
μ_D	Specific death rate	h^{-1}
μ_{max}	Maximum specific growth rate	h^{-1}
b	Back scattering fraction	-
c_N	Nitrate concentration	$g L^{-1}$
$c_{N,Feed}$	Nitrate concentration feed	$g L^{-1}$
D (D_i)	Desirability (for the i-th factor combination)	-
$D_{\Delta percentile}$	Desirability containing the scaled inverse of the width of the prediction band	-
D_{main}	Desirability containing the scaled expected response	-
E_a	Mass absorption coefficient	$m^2 kg^{-1}$
E_s	Mass scattering coefficient	$m^2 kg^{-1}$
$f()$	Function	-
F_M	Medium feed rate	$L h^{-1}$
F_S	Sample rate	$L h^{-1}$
h	Height	m
I_B	Incident light intensity	$\mu mol m^{-2} s^{-1}$
I_{avg}	Average light intensity	$\mu mol m^{-2} s^{-1}$
I_s	Light intensity of the light source	$\mu mol m^{-2} s^{-1}$
$I(z)$	Local light intensity	$\mu mol m^{-2} s^{-1}$
I_{max}	Maximum local light intensity	$\mu mol m^{-2} s^{-1}$
I_{min}	Minimum local light intensity	$\mu mol m^{-2} s^{-1}$
I_{opt}	Optimal local light intensity	$\mu mol m^{-2} s^{-1}$
I_0	Incident light intensity	$\mu mol m^{-2} s^{-1}$
i	index for factor combination	-
j	index for one of n chosen variables	-
k_a	Algal turbidity	$L g^{-1} m^{-1}$
K_I	Half-saturation concentration light	$\mu mol m^{-2} s^{-1}$
K_N	Uptake rate associated Monod kinetic constant	$g L^{-1}$
k_n	Non-algal turbidity	m^{-1}
L	Light duration (CSB) or depth of reactor (CSA)	h or m
pH	pH value (system)	-
pH_{min}	Minimum pH value	-
pH_{max}	Maximum pH value	-
pH_{opt}	Optimal pH value	-
q_N	Nitrate uptake rate	$g_{nitrate} g_{biomass}^{-1} h^{-1}$
R^2	Coefficient of determination	-
t	Time	h
V	Volume	L
w	Weighting factor in calculation of D	-
X (X_{max})	(Maximum) biomass concentration	$g L^{-1}$
y_i	Measured y value for the i-th data point	-
$y_{s,i}$	Simulated y value for the i-th data point	-
$\bar{Y}$	Mean of experimental values	-
$Y_{N/X}$	Ratio of maximum nitrate uptake rate and maximum specific growth rate	$g_{nitrate} g_{biomass}^{-1}$
z or D	Depth (system)	m

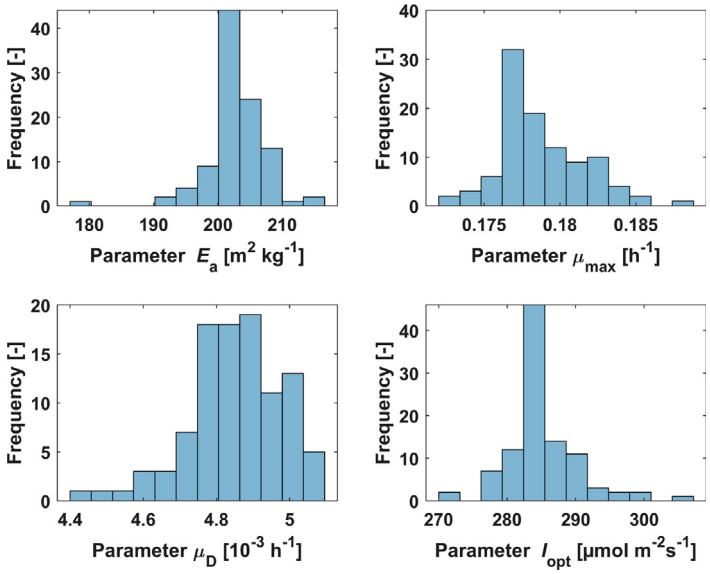

Fig. A1. Distribution of the estimated parameters of 100 randomly sampled and performed estimations for the parameters E_a, μ_{max}, μ_D and I_{opt} for the *D. pseudocommunis* model.

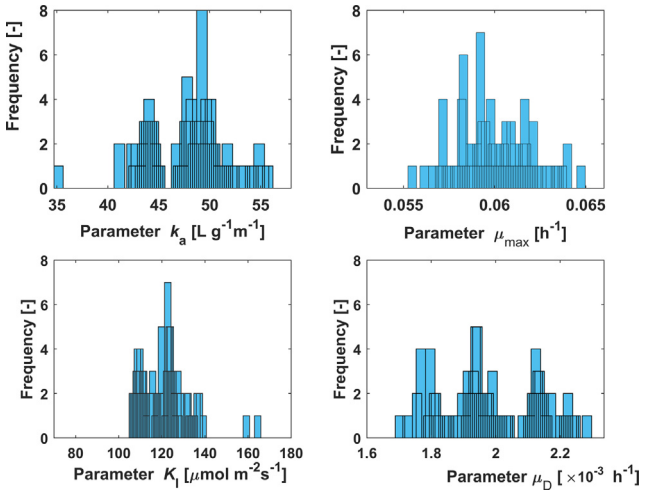

Fig. A2. Distribution of the estimated parameters of 100 randomly sampled and performed estimations for the parameters k_a, μ_{max}, K_I and μ_D for the first *C. vulgaris* model.

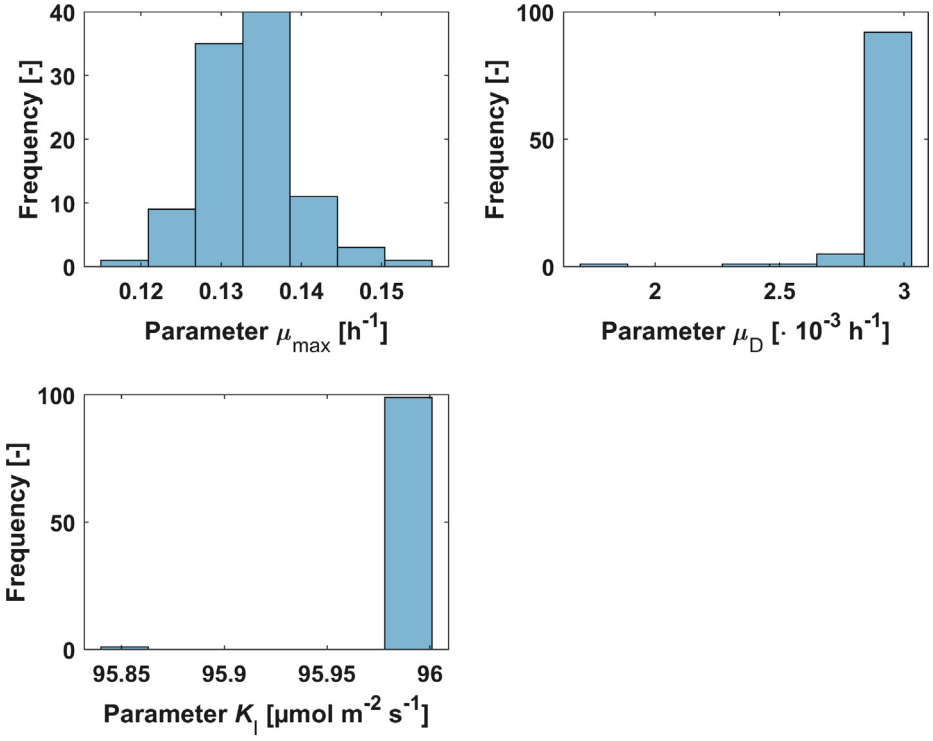

Fig. A3. Distribution of the estimated parameters of 100 randomly sampled and performed estimations for the parameters μ_{max}, μ_D and K_I for the improved *C. vulgaris* model.

References

Andersen, R.A. (Ed.), 2005. Algal culturing techniques. Amsterdam: Elsevier Acad. Press. URL www.academia.edu/28995029/Andersen_Algal_Culturing_Techniques.

Andrews, J.F., 1968. A mathematical model for the continuous culture of microorganisms utilizing inhibitory substrates. Biotechnol. Bioeng. 10, 707–723. https://doi.org/10.1002/bit.260100602.

Aslan, S., Kapdan, I.K., 2006. Batch kinetics of nitrogen and phosphorus removal from synthetic wastewater by algae. Ecol. Eng. 28, 64–70. https://doi.org/10.1016/j.ecoleng.2006.04.003.

Béchet, Q., Laviale, M., Arsapin, N., Bonnefond, H., Bernard, O., 2017. Modeling the impact of high temperatures on microalgal viability and photosynthetic activity. Biotechnol. Biofuels 10, 1–11. https://doi.org/10.1186/s13068-017-0823-z.

Béchet, Q., Shilton, A., Guieysse, B., 2013. Modeling the effects of light and temperature on algae growth: state of the art and critical assessment for productivity prediction during outdoor cultivation. Biotechnology advances 31, 1648–1663. https://doi.org/10.1016/j.biotechadv.2013.08.014.

Béchet, Q., Shilton, A., Guieysse, B., 2014. Full-scale validation of a model of algal productivity. Environmental science & technology 48, 13826–13833. https://doi.org/10.1021/es503204e.

Bischoff, H.W., Bold, H.C., 1963. Phycological studies IV. Some soil algae from Enchanted Rock and related algal species. Phycol. Stud. (University of Texas publication 6318).

Cataldo, D.A., Maroon, M., Schrader, L.E., Youngs, V.L., 1975. Rapid colorimetric determination of nitrate in plant tissue by nitration of salicylic acid. Commun. Soil Sci. Plant Anal. 6, 71–80. https://doi.org/10.1080/00103627509366547.

Chinnasamy, S., Ramakrishnan, B., Bhatnagar, A., Das, K.C., 2011. Biomass production potential of a wastewater alga Chlorella vulgaris arc1 under elevated levels of co_2 and temperature. Int. J. Mol. Sci. 10, 518–532. https://doi.org/10.3390/ijms10020518.

Concas, A., Lutzu, G.A., Pisu, M., Cao, G., 2012. Experimental analysis and novel modeling of semi-batch photobioreactors operated with chlorella vulgaris and fed with 100% (v/v) co2. Chem. Eng. J. 213, 203–213. https://doi.org/10.1016/j.cej.2012.09.119.

Cornet, J.-F., Dussap, C., Gros, J.-B., 1997. Kinetics and energetics of photosynthetic micro-organisms in photobioreactors. Advances in Biochemical Engeneering/Biotechnology 59, 154–222. https://doi.org/10.1007/BFb0102299.

Cornet, J.F., Dussap, C.G., 2009. A simple and reliable formula for assessment of maximum volumetric productivities in photobioreactors. Biotechnol. Prog. 2009, 424–435. https://doi.org/10.1002/btpr.138.

Del Rio-Chanona, E.A., Ahmed, N.R., Wagner, J., Lu, Y., Zhang, D., Jing, K., 2019. Comparison of physics-based and data-driven modelling techniques for dynamic optimisation of fed-batch bioprocesses. Biotechnol. Bioeng. 116, 2971–2982. https://doi.org/10.1002/bit.27131.

Eilers, P.H.C., Peeters, J.C.H., 1988. A model for the relationship between light intensity and the rate of photosynthesis in phytoplankton. Ecol. Model. 42, 199–215. https://doi.org/10.1016/0304-3800(88)90057-9.

Eze, V.C., Velasquez-Orta, S.B., Hernández-García, A., Monje-Ramírez, I., Orta-Ledesma, M., 2018. Kinetic modelling of microalgae cultivation for wastewater treatment and carbon dioxide sequestration. Algal Research 32, 131–141. https://doi.org/10.1016/j.algal.2018.03.015.

Fernández-Sevilla, J.M., Brindley, C., Jiménez-Ruíz, N., Acién, G., 2018. A simple equation to quantify the effect of frequency of light/dark cycles on the photosynthetic response of microalgae under intermittent light. Algal Research 35, 479–487. https://doi.org/10.1016/j.algal.2018.09.026.

Filali, R., Tebbani, S., Dumur, D., Isambert, A., Pareau, D., Lopes, F., 2011. Growth modeling of the green microalga chlorella vulgaris in an air-lift photobioreactor. IFAC Proceedings Volumes 44, 10603–10608. https://doi.org/10.3182/20110828-6-IT-1002.01955.

Gatamaneni, B.L., Orsat, V., Lefsrud, M., 2018. Factors affecting growth of various microalgal species. Enviromental Engineering Science 35, 1–12. https://doi.org/10.1089/ees.2017.0521.

Glassey, J., Gernaey, K.V., Clemens, C., Schulz, T.W., Oliveria, R., Striedner, G., Mandenius, C.-F., 2011. Process analytical technology (PAT) for biopharmaceuticals. Biotechnol. J. 6, 369–377. https://doi.org/10.1002/biot.201000356.

Gouveia, L., Oliveira, A.C., 2009. Microalgae as a raw material for biofuels production. Journal of industrial microbiology & biotechnology 36, 269–274. https://doi.org/10.1007/s10295-008-0495-6.

Griffiths, M.J., Dicks, R.G., Richardson, C., Harrison, S.T.L., 2011. Advantages and challenges of microalgae as a source of oil for biodiesel. In: Liu, J., Chen, F., Huang, J. (Eds.), Microalgae as Feedstocks for Biodiesel Production. INTECH Open Access Publisher, pp. 119–123. https://doi.org/10.5772/30085.

He, L., Subramanian, V.R., Tang, Y.J., 2012. Experimental analysis and model-based optimization of microalgae growth in photo-bioreactors using flue gas. Biomass Bioenergy 41, 131–138. https://doi.org/10.1016/j.biombioe.2012.02.025.

Ifrim, G.A., Titica, M., Cogne, G., Boillereaux, L., Legrand, L., Caraman, S., 2014. Dynamic pH Model for Autotrophic Growth of Microalgae in Photobioreactor: A Tool for Monitoring and Control Purposes. AIChe Journal 60, 585–599. https://doi.org/10.1002/aic.14290.

Ifrim, G.A., Titica, M., Deppe, S., Frahm, B., Barbu, M., Caraman, S., 2019. Multivariable control strategy for the photosynthetic cultures of microalgae. In: 23rd International Conference on System Theory, Control and Computing (ICSTCC), pp. 218–223. https://doi.org/10.1109/ICSTCC.2019.8886109.

Jayaraman, S.K., Rhinehart, R.R., 2015. Modeling and optimization of algae growth. Industrial & Engineering Chemistry Research 54, 8063–8071. https://doi.org/10.1021/acs.iecr.5b01635.

Kessler, E., Czygan, F.-C., 1970. Physiologische und biochemische beiträge zur taxonomie der gattung chlorella. Arch. Mikrobiol. 70, 211–216. https://doi.org/10.1007/BF00407711.

Koller, A. (2017). Reaktionskinetik des lichtabhängigen Wachstums von Scenedesmus spec. in Flachplattenphotobioreaktoren. Dissertation TU München München. http://mediatum.ub.tum.de/?id=1328776.

Kuchemüller, K.B., Pörtner, R., Möller, J., 2020. Efficient optimization of process strategies with model-assisted design of experiments. In: Animal Cell Biotechnology: Methods and Protocols. Springer, US, pp. 235–249. https://doi.org/10.1007/978-1-0716-0191-4_13.

Kuhfuß, F., Gassenmeier, V., Deppe, S., Ifrim, G., Hernández Rodríguez, T., Frahm, B., 2022. View on a mechanistic model of chlorella vulgaris in incubated shake flasks. Bioprocess Biosyst. Eng.. https://doi.org/10.1007/s00449-021-02627-2.

Lee, E., Jalalizadeh, M., Zhang, Q., 2015. Growth kinetic models for microalgae cultivation: A review. Algal Research 12, 497–512. https://doi.org/10.1016/j.algal.2015.10.004.

Mairet, F., Titica, M., Bernard, O., Pruvost, J., 2010. Coupling biological and radiative models to describe microalgal growth in a photobioreactor. IFAC Proceedings Volumes 43, 168–173. https://doi.org/10.3182/20100707-3-BE-2012.0007.

Mallick, N., Mandal, S., Singh, A.K., Bishai, M., Dash, A., 2011. Green microalgae Chlorella vulgaris as potential feedstock for biodiesel. Journal of Chemical Technology & Biotechnology 87, 137–145. https://doi.org/10.1002/jctb.2694.

Mandalam, R.K., Palsson, B., 1998. Elemental balancing of biomass and medium composition enhances growth capacity in high-density chlorella vulgaris cultures. Biotechnology and bioengineering 59, 605–611. https://doi.org/10.1002/(SICI)1097-0290(19980905)59:5<605::AID-BIT11>3.0.CO;2-8.

Matos, A.P., Ferreira, W.B., de Oliveira Torres, R.C., Morioka, L.R.I., Canella, M.H.M., Rotta, J., da Silva, T., Moecke, E.H.S., Sant'Anna, E.S., 2015. Optimization of biomass production of chlorella vulgaris grown in desalination concentrate. J. Appl. Phycol. 27, 1473–1483. https://doi.org/10.1007/s10811-014-0451-y.

Miazek, K., Ledakowicz, S., 2013. Chlorophyll extraction from leaves, needles and microalgae: A kinetic approach. Int J Agric & Biol Eng 6, 107–115. https://doi.org/10.3965/j.ijabe.20130602.0012.

Mirzaie, M.A., Kalbasi, M., Ghobadian, B., Mousavi, S.M., 2016. Kinetic modeling of mixotrophic growth of chlorella vulgaris as a new feedstock for biolubricant. J. Appl. Phycol. 28, 2707–2717. https://doi.org/10.1007/s10811-016-0841-4.

Möller, J., Hernández Rodríguez, T., Müller, J., Arndt, L., Kuchemüller, K.B., Frahm, B., Eibl, R., Eibl, D., Pörtner, R., 2020. Model uncertainty-based evaluation of process strategies during scale-up of biopharmaceutical processes. Computers & Chemical Engineering 134, 106693. https://doi.org/10.1016/j.compchemeng.2019.106693.

Möller, J., Kuchemüller, K.B., Steinmetz, T., Koopmann, K.S., Pörtner, R., 2019. Model-assisted design of experiments as a concept for knowledge-based bioprocess development. Bioprocess and biosystems engineering 42, 867–882. https://doi.org/10.1007/s00449-019-02089-7. Springer.

Morschett, H., Schiprowski, D., Rohde, J., Wiechert, W., Oldiges, M., 2017. Comparative evaluation of phototrophic microtiter plate cultivation against laboratory-scale photobioreactors. Bioprocess and biosystems engineering 40, 663–673. https://doi.org/10.1007/s00449-016-1731-5.

Moser, A., Kuchemüller, K.B., Deppe, S., Hernández Rodríguez, T., Frahm, B., Pörtner, R., Hass, V.C., Möller, J., 2021. Model-assisted doe software: optimization of growth and biocatalysis in Saccharomyces cerevisiae bioprocesses. Bioprocess Biosyst. Eng. 2021, 1–18. https://doi.org/10.1007/s00449-020-02478-3.

Pegallapati, A.K., Nirmalakhandan, N., 2012. Modeling algal growth in bubble columns under sparging with CO_2-enriched air. Bioresour. Technol. 124, 137–145. https://doi.org/10.1016/j.biortech.2012.08.026.

Qiu, R., Gao, S., Lopez, P.A., Ogden, K.L., 2017. Effect of ph on cell growth, lipid production and co_2 addition of microalgae Chlorella sorokiniana. Algal Research 28, 192–199. https://doi.org/10.1016/j.algal.2017.11.004.

Spiess, A.-N., Neumeyer, N., 2010. An evaluation of R^2 as an inadequate measure for nonlinear models in pharmacological and biochemical research: a Monte Carlo approach. BMC pharmacology 10, 6. https://doi.org/10.1186/1471-2210-10-6.

von Stosch, M., Hamelink, J., Oliveira, R., 2016. Hybrid modeling as a QbD/PAT tool in process development: an industrial E. coli case study. Bioprocess and biosystems engineering 39, 773–784. https://doi.org/10.1007/s00449-016-1557-1. Springer.

Tamiya, H., Iwamura, T., Shibata, K., Hase, E., Nihei, T., 1953. Correlation between photosynthesis and light-independent metabolism in the growth of Chlorella. BIOCHIMICA ET BIOPHYSICA ACTA 12, 23–40. https://doi.org/10.1016/0006-3002(53)90120-6.

Tao, R., Bair, R., Lakaniemi, A., van Hullebusch, E.D., Rintala, J.A., 2020. Use of factorial experimental design to study the effects of iron and sulfur on growth of Scenedesmus acuminatus with different nitrogen sources. J. Appl. Phycol. 32, 221–231. https://doi.org/10.1007/s10811-019-01915-5.

Vanags, J., Kunga, L., Dubencovs, K., Galvanauskas, V., Grigs, O., 2015. Influence of Light Intensity and Temperature on Cultivation of Microalgae Desmodesmus Communis in Flasks and Laboratory-Scale Stirred Tank Photobioreactor. Latvian Journal of Physics and Technical Sciences 52, 59–70. https://doi.org/10.1515/lpts-2015-0012.

Wellburn, A.R., 1994. The Spectral Determination of Chlorophylls a and b, as well as Total Carotenoids, Using Various Solvents with Spectrophotometers of Different Resolution. J. Plant Physiol. 1994, 307–313. https://doi.org/10.1016/S0176-1617(11)81192-2.

Wong, Y.K., Ho, K.C., Tsang, Y.F., Wang, L., Yung, K.K.L., 2016. Cultivation of Chlorella vulgaris in Column Photobioreactor for Biomass Production and Lipid Accumulation. Water environment research: a research publication of the Water Environment Federation 88, 40–46. https://doi.org/10.2175/106143015X14362865227553.

Yun, Y.S., Park, J.M., 2003. Kinetic modeling of the light-dependent photosynthetic activity of the green microalga Chlorella vulgaris. Biotechnol. Bioeng. 83, 303–311. https://doi.org/10.1002/bit.10669.

Zhang, D., Del Rio-Chanona, E.A., Petsagkourakis, P., Wagner, J., 2019. Hybrid physics–based and data–driven modeling for bioprocess online simulation and optimization. Biotechnol. Bioeng. 157, 293. https://doi.org/10.1002/bit.27120.

Zhang, D., Wan, M., Rio-Chanona, E.A.D., Huang, J., Wang, W., Li, Y., Vassiliadis, V.S., 2016. Dynamic modelling of Haematococcus pluvialis photoinduction for astaxanthin production in both attached and suspended photobioreactors. Biotechnol. J. 13, 69–78. https://doi.org/10.1016/j.algal.2015.11.019.

Zhao, Y., Yue, C., Geng, D., Ning, S., Ma, T., Yu, X., 2019. Role of media composition in biomass and astaxanthin production of Haematococcus pluvialis under two-stage cultivation. Bioprocess Biosyst Eng. 42, 593–602. https://doi.org/10.1007/s00449-018-02064-8.